

# Optimization of the experimental parameters of the ligase cycling reaction

Niels Schlichting, Felix Reinhardt, Sven Jager, Michael Schmidt, Johannes Kabisch \*

Department of Biology, TU Darmstadt, Schnittspahnstraße 12, DE-64287, Germany.

Received xx, 2019; Revised x, 2019; Accepted xx, 2019

## ABSTRACT

The ligase cycling reaction (LCR) is a scarless and efficient method to assemble plasmids from fragments of DNA. This assembly method is based on the hybridization of DNA fragments with complementary oligonucleotides, so-called bridging oligos (BOs), and an experimental procedure of thermal denaturation, annealing and ligation. In this study, we explore the effect of molecular crosstalk of BOs and various experimental parameters on the LCR by utilizing a fluorescence-based screening system. The results indicate an impact of the melting temperatures of BOs on the overall success of the LCR assembly. Secondary structure inhibitors, such as DMSO and betaine, are necessary for assemblies made of large parts (>350 bp) whereas they show negative effects for assemblies with mixtures of small and large parts. Adjustments of the annealing, ligation and BO-melting temperature are useful but depend on the sizes of the DNA fragments. Based on this, a step-by-step protocol is offered within this study to ensure a transferable routine for high efficient LCR assemblies.

## INTRODUCTION

It is the goal of synthetic biology to specify, design, build and test genetic circuits, and this goal requires rapid prototyping approaches to facilitate assembly and testing of a wide variety of circuits. To this end, many assembly methods were used in the last decades to build DNA constructs, e.g., Gibson assembly (1), Golden Gate assembly (2, 3), circular polymerase extension cloning (CPEC, 4), biopart assembly standard for idempotent cloning (BASIC, 5) and yeast homologous recombination (YHR, 6). Some of these methods require specific modifications of the DNA parts such as overhangs or restriction sites, which hamper the reusability, while other methods are slow or leave scars. Additionally, DNA part standardization approaches, e.g. the BioBrick-system, result in sequence redundancies which have a negative impact on assembly efficiencies (7).

By contrast, the ligase cycling reaction (LCR) fulfills the prerequisites for automated assemblies and uses phosphorylated DNA parts (8, 9, 10, 11). The assembly order is determined by single-stranded oligonucleotides

building a bridge (so-called bridging oligonucleotides, BOs) between adjacent parts. Bridging oligos are typically designed by the scientists, based on general rules provided by the literature (8, 9). One important parameter for the LCR-assembly is the melting temperature ( $T_m$ ) of the BOs at around 70 °C for each half to facilitate optimal hybridization of template and oligonucleotide for given cycling parameters. Closely related is the free energy  $\Delta G$ , which is assumed as the more important quantity for oligonucleotide-based biological experiments (12, 13). In the LCR, this impact is counteracted by using dimethyl sulfoxide (DMSO) and betaine to increase  $\Delta G$  and thus to reduce secondary structures (8, 9). Nevertheless, the role of  $\Delta G$ -related crosstalk and the potential of  $\Delta G$ -optimized BOs in the LCR has not been investigated so far.

The literature offers several tools regarding LCR optimization. Nowak et al. (14) provides a tool for the assembly of DNA that codes for a protein, where they return both the DNA fragments as well as the BOs to minimize unwanted effects. The tool considers codon mutations, as long as they encode the same amino acid, and is intended to be applied for LCR-based gene synthesis. Bode et al. (15) offers similar functionality. Another web-application includes the design of primers and performs  $T_m$  and  $\Delta G$  cross-checks for the oligonucleotide sequences against themselves, their DNA probes and whole genomes (12) but is not applied for the LCR. Robinson et al. (16) use a BO-design-tool with an adjustable target melting temperature but without optimizing the crosstalk. An experimental perspective is given by de Kok et al. (9), where a design-of-experiment approach and multivariate data analysis were used to assess the impact of a wide range of parameters including the concentrations of the secondary structure inhibitors DMSO and betaine. The following study starts with these baseline-conditions. The LCR is investigated with the scope on the impact of the choice of BOs, their intramolecular and intermolecular crosstalk and the context of the experimental temperatures. For this, a toy-model plasmid and fluorescence-based readout is utilized (graphical abstract: Figure 1) to detect and validate the influence of all parameters and to generate new rules for an optimized LCR-assembly.

\*To whom correspondence should be addressed. Tel: +49 6151 1622044; Email: johannes@kabisch-lab.de

2, 2019, Vol. xx, No. xx

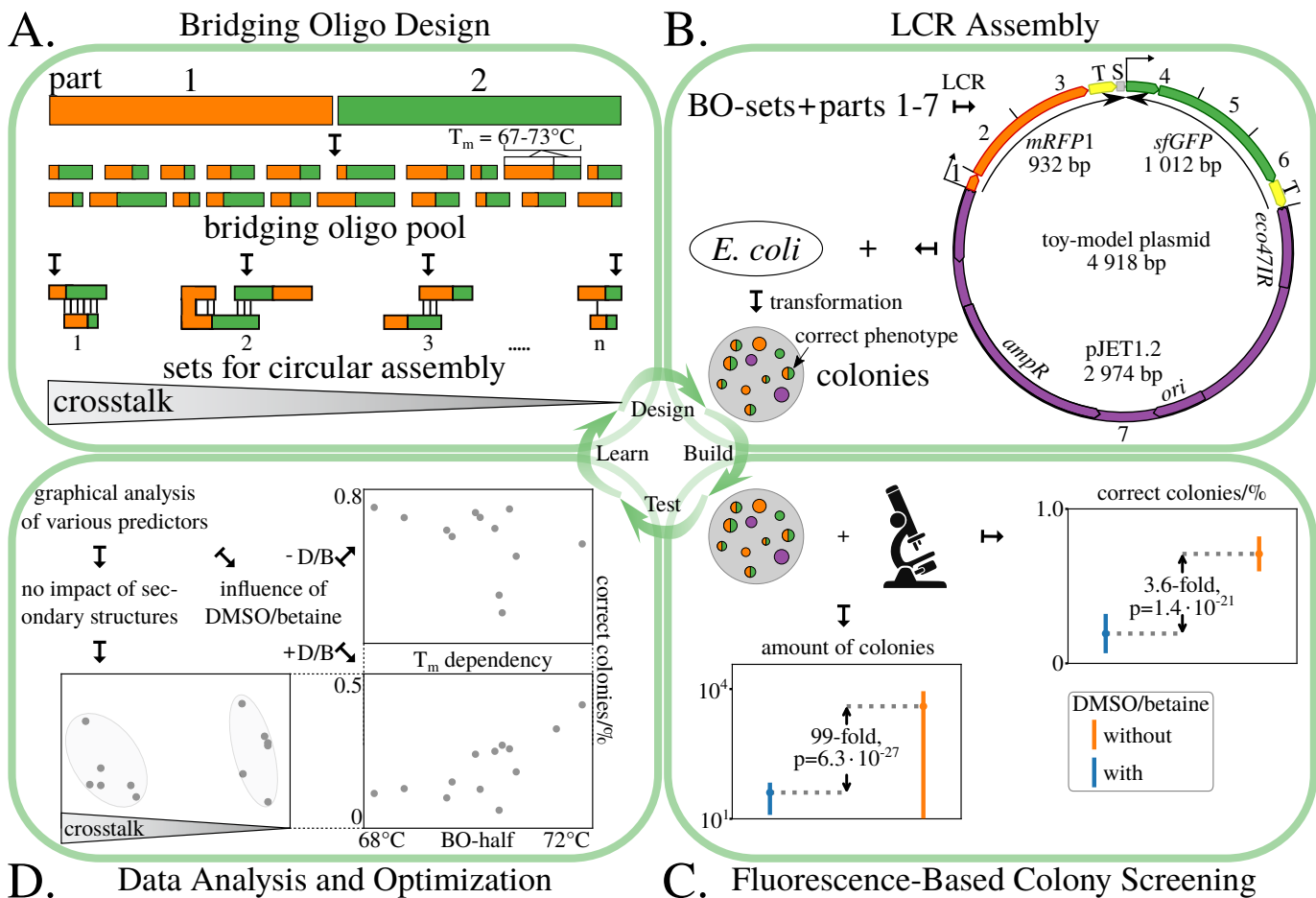


**Figure 1.** Workflow for the LCR optimization. **A.** Bridging oligo-sets (BO-sets) were designed using general design rules with the focus on  $\Delta G$ -related BO-crosstalk while maintaining a  $T_m$  of  $70 \pm 3^\circ\text{C}$ . **B.** In total, 25 sets were designed, including one manually designed set using the software *Primer3*, and utilized for the LCR-assembly of a toy-model plasmid. The plasmid consists of seven parts with lengths in the range of 79 bp to 2974 bp and a total length of 4918 bp. It contains two genes for fluorescent proteins, *mRFP1* and *sfGFP*, and a vector. Both fluorescent protein genes were split into three subparts (*mRFP1*: parts 1-3, *sfGFP*: parts 4-6). The same terminator *Bba\_B0015* (T) was used twice to simulate sequence redundancies. A DNA-spacer S (37 bp) was added at the end of part 3 to avoid hybridization of the BO utilized for the ligation of parts 6 and 7. The sequences of all parts are shown in Supplementary Table S1. **C.** The toy-model plasmid enables a fast and reliable fluorescence-based readout to observe the LCR efficiency and the total amount of colonies to investigate various LCR conditions. Based on this method, a significant negative impact by using the baseline-LCR conditions (8% v/v DMSO, 0.45 M betaine) was revealed for the seven-part toy-plasmid. The p-values were derived from a Kolmogorov-Smirnov test between the two sets of data shown in Figure Supplementary Figure S1. **D.** With the focus on all BO-sets, no  $\Delta G$ -related impact was detected in the baseline and DMSO/betaine-free LCR conditions. Further graphical analysis of the BO-sets revealed an association of the average BO- $T_m$ , the efficiency and total amount of colonies. Finally, the optimizations were applied on another split of the toy-plasmid (three-part design: 1. *mRFP1*, 2. *sfGFP*, 3. vector). *ampR*: gene for ampicillin resistance,  $\pm D/B$ : with or without DMSO and betaine, *eco47IR*: gene for a restriction enzyme (reduction of religations of the vector), *mRFP1*: monomeric red fluorescent protein 1, *ori*: origin of replication, *sfGFP*: superfolder green fluorescent protein,  $T_m$ : melting temperature.

## MATERIALS AND METHODS

### Toy-model plasmid

All LCRs were performed with a toy-model plasmid made of seven fragments (Figure 1B), with a total length of 4918 bp. This plasmid consists of six inserts and the plasmid cloning vector CloneJet pJET1.2/blunt (2974 bp; Thermo Fischer Scientific, Massachusetts, USA). For the inserts, two genes of fluorescent proteins, *sfGFP*, *mRFP1*, were ordered at Addgene ([www.addgene.org](http://www.addgene.org); pYTK001, pYTK090; 17) and split into three subparts each to increase size heterogeneity, so that the plasmid fragment length ranges from 79 bp to 2974 bp. Additionally, the same terminator *Bba\_B0015* was used in both fluorescent protein genes to further increase assembly complexity. Due to this sequence homology, a spacer sequence

of 37 bp was added at the 3'-end of part 3 to prevent the ligation with part 7. For all *in silico* cloning, the software Geneious was utilized (v. 11.0.5, <http://www.geneious.com>, 18).

### Part amplification

Primers for the amplification (Eurofins Genomics, Ebersberg, Germany) were phosphorylated by the T4-polynucleotidekinase/-buffer (New England Biolabs, Ipswich, USA) prior to amplification *via* PCR (Q5<sup>®</sup> High-Fidelity Polymerase, New England Biolabs, Ipswich, USA). Forward and reverse primers were phosphorylated separately in a total volume of 50  $\mu\text{L}$ , a primer-concentration of 1  $\mu\text{M}$ , 2 mM ATP and 10 U of T4-PNK for 1 h at  $37^\circ\text{C}$  and 20 min at  $65^\circ\text{C}$  for the denaturation. The low primer concentration was chosen

because it is beneficial for the enzymatic phosphorylation. The 79 bp promoter of *mRFP1* (part 1, Figure 1B) was ordered as forward and reverse strand (lyophilized, salt-free). Both strands were phosphorylated separately, as described for the amplification primers followed by an annealing procedure to obtain double-stranded DNA (3 min at 95 °C and 70 cycles of 20 s with an incremental decrease of 1 °C). The vector pJET1.2/blunt was PCR-amplified using a template suitable to detect plasmid-carryover by blue-white screening (pJET1.2/blunt+*lacZ*). Prior to amplification of the vector, the pJET1.2/blunt-*lacZ* plasmid was linearized by restriction digestion (restriction site in the *lacZ*). Afterwards, all PCR products were DpnI-digested (60 min at 37 °C; inactivation: 20 min at 80 °C), purified (column-based NEB Monarch<sup>®</sup> PCR & DNA Cleanup Kit; New England Biolabs, Ipswich, USA) and the DNA quantity/quality was measured by photometry (Spectrophotometer UV5Nano, Mettler Toledo, Columbus, USA). Afterwards, the phosphorylated primers and DNA parts were stored at -20 °C. The sequences of all amplification primers are shown in Supplementary Table S2. The sequences of the toy-model parts are shown in Supplementary Table S1.

### Bridging oligo design

Bridging oligos were predicted according to the rules given in de Kok et al. (9): they were all orientated in forward direction and designed at specific ingredient concentrations of 10 mM Mg<sup>2+</sup>, 50 mM Na<sup>+</sup>, 3 nM plasmid parts, 30 nM BOs and 0 mM dNTPs. All BOs were ordered lyophilized from Eurofins Genomics (Ebersberg, Germany) as salt-free custom DNA oligonucleotides. Quality was checked by Eurofins Genomics *via* matrix-assisted laser desorption ionization-time of flight (MALDI-TOF) or capillary electrophoresis (CE).

One BO-set was designed manually with the melting temperature tool of Primer3 (19), which is distributed with the software suite Geneious. For the  $T_m$  calculation and salt correction, the nearest-neighbor algorithm and the corresponding salt correction by SantaLucia (20) were utilized to design a BO-set with melting temperatures of 70 °C for each half-BO. Primer3 only accepts a single DNA concentration, despite the experiment using different concentrations of parts and BOs. As prompted by Geneious, only the BO concentration of 30 nM was inputted. This manual set is denoted by an "M".

To investigate the crosstalk of BOs, more sets were designed by minimizing or maximizing  $\Delta G$ -dependent crosstalk between oligonucleotides while maintaining a  $T_m$  between 67 °C and 73 °C. Crosstalk is defined as the sum of all minimum free energies (MFES) when cofolding each oligonucleotide of a BO-set with each oligonucleotide in that set and with itself. As a reference temperature for the crosstalk calculations, the annealing temperature of the multi-step LCR protocol was used (55 °C, 9). As with the manual set, the SantaLucia parameters were utilized for the  $T_m$  calculations. Additionally, the DNA part concentration was adjusted to 3 nM to match the experiment. The impact of DMSO and betaine were not considered for the calculations of the MFES. Sets with minimized crosstalk are denoted by "L" for low crosstalk and sets with maximized crosstalk by a "H" for high

crosstalk. All BO-sets, sequences and melting temperatures are provided in Supplementary Table S3.

### Ligase cycling reaction

For the assembly, the purified PCR products were mixed with supplements with the following concentrations: 1 × ligase buffer, 0.5 mM NAD<sup>+</sup>, 3 nM of toy-plasmid parts 1-6, 0.45 M betaine and 8 % -v/v DMSO. In contrast to de Kok et al. (9), the concentration of the vector pJET1.2/blunt (part 7) was reduced to 0.3 nM to achieve fewer religations of the vector. LCRs using these experimental concentrations are called baseline-conditions. The 10×-Ampligase<sup>®</sup> reaction buffer was self-made with the concentrations described by the manufacturer of the Ampligase<sup>®</sup> (Lucigen, Wisconsin, USA). NAD<sup>+</sup> was supplied separately by using a self-prepared 10 mM stock solution. Bridging oligo sets were premixed in nuclease-free water with 1.5 μM of each BO, heated up for 10 min at 70 °C and cooled down on ice before adding them to the split master-mixes. Subsequently 10 U of Ampligase<sup>®</sup> (Lucigen, Wisconsin, USA) was added. After rigorous mixing and centrifugation, each LCR was split in at least three ( $n=3$ ) reactions with a cycling-volume of 3 μL. The results presented in Figure 2 and Supplementary Figure S7 were based on LCR-quintuplets ( $n=5$ ) and show the impacts of utilizing or omitting DMSO and betaine. After the cycling, all LCRs were cooled down on ice to recondense evaporated liquid in the PCR-tubes, and centrifuged.

For the cycling, a DNA Engine Tetrad<sup>®</sup>2 thermal cycler, 96-well Alpha<sup>™</sup> Unit cycling block and low-profile PCR stripes (Bio-Rad Laboratories GmbH, Muenchen, Germany) were utilized. The speed of ramping used for all LCRs was 3 °C s<sup>-1</sup>. The cycling was initiated by a denaturation step at 94 °C for 2 min, followed by 25 cycles at 94 °C for 10 s, 55 °C for 30 s and 66 °C for 1 min. In contrast to the published protocols (8, 9), 25 cycles instead of 50 cycles were used due to the low total LCR volume of 3 μL. Afterwards, 30 μL electro-competent or chemically-competent NEB<sup>®</sup> 10-β *E. coli* cells (self-made batches; New England Biolabs, Ipswich, USA) were mixed with each LCR and the total volume was transferred to cuvettes for electroporation with a diameter of 1 mm. The transformations were performed by applying an electric pulse of 2.5 kV or by using 96-well PCR-plates and a cycling block for the heat-shock. For the heat-shock, the 96-well plates were put on ice for 30 min, then heat-shocked for 30 s at 42 °C, then put on ice again for 10 min. After the recovery at 37 °C for 1 h in 470 μL SOC medium (chemical transformation: 170 μL), an appropriate volume of the transformation mix was plated on Lysogeny Broth (Miller) plates containing 1 % -m/v agar and 100 μg mL<sup>-1</sup> ampicillin, which were grown for 15 h at 37 °C.

Electroporations were performed serially for each single LCR: 1. cells were mixed from a master-aliquot for each experiment with one LCR-replicate of one LCR condition, 2. suspension was transferred to a cuvette, 3. an electric pulse was applied, 4. SOC-medium was added, 5. the cell-suspension was transferred to a tube, 6. the tube was put in a thermal cycler for recovery and 7. finally the suspension was plated on agar plates. Each LCR condition was transformed in a non-batch-wise manner to reduce workflow-derived influences, so that, e.g., each condition was transformed once



before proceeding with the second replicates. For chemical transformations, the experiments were performed in a more parallel manner: 1. cells were mixed from a master-aliquot for each experiment with all replicates of all LCRs in a 96-well plate using a multi-channel pipette, 2. the suspensions were incubated on ice, 3. the heat-shock was applied in a PCR-cycler, 4. the suspensions were put on ice, 5. SOC-medium was added to all LCR-cell-mixes followed by the recovery and plating.

### Colony screening and plasmid sequencing

By transforming the LCRs into *E. coli*, the toy-model plasmid enables a fluorescence-based discrimination of correct (red-fluorescent and green-fluorescent CFUs) and misligated plasmids (red or green or non-fluorescent CFUs). To investigate the LCR assembly, the efficiencies of all LCRs were determined by observing the phenotype of ampicillin-resistant CFUs *via* fluorescence microscopy (microscope: Axio Vert.A1, Carl Zeiss Microscopy GmbH, Jena, Germany, 50 $\times$ -magnification; LEDs for sfGFP/mRFP1: 470/540–580 nm). To calculate the LCR efficiency, the phenotypes of all CFUs per LCR were screened. For plates with more than 100 CFUs, 100 colonies were screened randomly by first picking the spot of interest macroscopically followed by the observation with the microscope. The efficiency was obtained by dividing the number of correct CFUs by the total number of observed CFUs. The amount of CFUs per 3  $\mu$ L was obtained from the total CFUs per plate and the used plating volume and dilution.

To validate this fluorescence-based system, plasmids from 120 CFUs with different phenotypes were isolated with the Monarch<sup>®</sup> Plasmid Miniprep Kit (New England Biolabs, Ipswich, USA) and analyzed *via* Sanger-sequencing (Eurofins Genomics, Ebersberg, Germany) to correlate them with the genotypes.

### Graphical analysis

Unless specified otherwise,  $T_m$  calculations in the following sections were performed with the thermodynamic parameters and salt correction by SantaLucia (20) and the divalent salt conversion by von Ahsen et al. (21). The shown  $T_m$ s are of half-BOs. Each half-BO is complementary to the DNA part that is designed to attach to. A BO is the direct concatenation of two half-BOs. Dangling ends and coaxial stacking were not included in the calculation. Error bars are the standard deviation with Bessel's correction. The average  $T_m$  of a BO-set is obtained from all half-BOs of the set.

## RESULTS AND DISCUSSION

### Toy-Model Plasmid Offers Robust System to Investigate LCR Assemblies

To simulate a challenging SynBio-construct for the investigations of the LCR, a toy-model plasmid was designed (Figure 1B). This plasmid consists of seven parts of varying size (79 bp to 2974 bp) and the same BioBrick terminator sequence *BBa\_B0015* in both fluorescent protein genes. To investigate the LCR, different bridging oligo sets, experimental parameters, a toy-model plasmid and

fluorescence-based analysis were used. For the analysis and optimization, ~100 CFUs/LCR (if available) were screened *via* fluorescence microscopy to calculate the efficiency of each assembly reaction. The amount of CFUs per 3  $\mu$ L LCR was determined by macroscopic counting of all colonies per agar plate and extrapolation by using the dilution-factor. In total, 61 different experimental conditions were tested and more than 15000 colonies were screened by fluorescence-microscopy to obtain the assembly efficiencies. In contrast to the vector concentration of 3 nM in the literature (8, 9), the concentration was decreased to 0.3 nM to counteract religations. Positive effects of increasing the molar insert-to-vector ratio were already described for other cloning methods (22, 23) and were confirmed in preliminary LCRs (data not shown).

No fluorescent CFUs were obtained in the control reactions without the ligase (Figure 2). Additionally, blue-white screening of about 1000 non-fluorescent CFUs revealed no carry-over of the template used for the amplification of the vector pJET1.2/blunt. A carry-over of the templates pYTK001 or pYTK090 used for the amplification of *sfGFP* and *mRFP1* was not possible due to a change of the antibiotic resistance marker gene.

To validate the fluorescence-based readout, the observed phenotypes of 120 CFUs with different phenotypes were correlated with the corresponding plasmids *via* Sanger-sequencing. The analyzed plasmids from 60 CFUs with a bicolored fluorescence (red and green) contained all seven DNA parts in the correct order/orientation when compared with the *in silico* sequence of the toy-plasmid. Sequencing results of 60 plasmids with a different phenotype (20 plasmids from only green fluorescent CFUs, 20 plasmids from only red fluorescent CFUs and 20 plasmids from non-fluorescent CFUs) indicated that they lacked at least one *sfGFP*-subpart or *mRFP1*-subpart (still red or green) or were religated vector (no fluorescence). The latter phenotype was also observed for plasmids with missing subparts of both fluorescent protein genes in preliminary experiments. Point-mutations in the LCR products were regarded as errors introduced by amplification primers, PCRs or *E. coli* and were not treated as LCR-misassemblies.

Within our experiments, the misassembled plasmids from green fluorescent colonies lacked at least one subpart of the *mRFP1*. Interestingly, about 10 bp to 100 bp of both ends of the missing subparts were still existent. For the 20 analyzed CFUs with only the red fluorescent phenotype, the plasmids lacked the spacer sequence at the 3'-end of the *mRFP1* and the entire *sfGFP*. This suggests that *E. coli* can recognize the 129 bp *BBa\_B0015* terminator that is used for both *sfGFP* and *mRFP1* and delete it by *recA*-independent recombination (24, 25). Related to this, the BO that spans parts 6 and 7 can partly hybridize with the terminator in part 3 and may negatively influence the ligation.

Another issue is related to the heterogeneous LCR-mixture, which contains the desired DNA fragments, debris of these fragments from PCRs, amplification primers and PCR templates (even if they are digested and purified). *E. coli* may circularize any linear DNA in the mixture. The subsequent transformation of *E. coli* enables a ring closure by endogenous mechanisms and the growth of CFUs containing the religated vector or plasmids with missing parts. This was observed in

the control reaction without ligase in Figure 2. Thus the carry-over of DNA in combination with the ability of *E. coli* to ligate linear DNA contributes both to the amount of misassembled plasmids and correct plasmids.

In summary, the fluorescence-based screening of colonies employed here is a valid and fast (manually:  $\sim 500$  CFUs  $\text{h}^{-1}$ ) method to determine the assembly efficiencies and to investigate the influence of changing parameters in the LCR. A correlation of the phenotype and genotype is a useful tool without the need for next generation sequencing and offers an objective true-false readout by microscopy (as utilized for these studies) or photometric analysis of images (using e.g. OpenCFU, 26; CellProfiler, 27).

### Influence of DMSO, betaine and the $T_m$ of bridging oligos on LCR assemblies

Thirteen different BO-sets, with sequences given in Supplementary Table S4, were used to assemble the toy-model plasmid made of seven fragments. Two separate experiments were performed with different conditions. The baseline-LCR used 8%  $v/v$  DMSO and 0.45 M betaine, whereas the crosstalk-increased LCR did not use any DMSO or betaine.

On average, the LCRs with both detergents revealed  $3.6\times$  lower efficiencies and  $99\times$  fewer total CFUs per  $3\mu\text{L}$  in comparison to assemblies without DMSO and betaine ( $p < 0.001$ , Figure 1C; raw data in Supplementary Figure S1). Further confirmation of these results can be seen in Supplementary Figure S7 and Supplementary Figure S9 in more consistent experiments using the same batches of DNA-parts and competent cells. Graphical analysis of various predictors revealed no  $\Delta G$ -related effects for assembling the toy-plasmid for both experimental setups (Figure 3A and 3B; more predictors in Supplementary Figure S2, Supplementary Figure S3, Supplementary Figure S4 and Supplementary Figure S5). Guanosine or cytosine were not found to be necessary at the 3'-end of BOs.

For LCRs with DMSO and betaine, BO-related differences were detected, e.g., the LCR using BO-set L1 was less efficient than using H1 (Figure 2A). Further analysis of the used BO-sets revealed an impact of the melting temperature despite the  $T_m$ s of all sets being similar and found in the range from  $68^\circ\text{C}$  to  $72^\circ\text{C}$  (Figure 3C). Sets with a BO- $T_m$  of  $68^\circ\text{C}$  were found to have 10% efficiency whereas sets with a BO- $T_m$  of  $72^\circ\text{C}$  were found to have 50% efficiency. This suggests that a melting temperature higher than  $72^\circ\text{C}$  may result in even better assemblies for LCRs with DMSO and betaine. This is confirmed by recalculating the melting temperatures of the set of sequences designed to have a  $T_m$  of  $70^\circ\text{C}$  by de Kok et al. (9), who used the SantaLucia parameters with the salt correction by Owczarzy et al. (28). We have found the average  $T_m$  of these half-BOs to be  $72.2^\circ\text{C}$  when calculated using these parameters. When using the SantaLucia parameters and SantaLucia salt correction as has been done so far in this study, the  $T_m$  is found at  $74.8^\circ\text{C}$ . The impact of different salt corrections is illustrated in Supplementary Figure S6. Overall, for LCRs with 8%  $v/v$  DMSO and 0.45 M betaine, a BO target temperature above  $70^\circ\text{C}$  was found to be beneficial.

Investigation of the Primer3 source code used for the design of the manual BO-set and comparison with SantaLucia

(20) revealed that the code expects both concentrations to be identical and to sum up to the input amount. Thus the prompted BO concentration of 30 nM corresponds to part and BO concentrations of 15 nM. Due to this, the manual BO-set had an average  $T_m$  of  $71.5^\circ\text{C}$  (Figure 3) when evaluated in full accordance with the SantaLucia formula instead of the targeted  $70^\circ\text{C}$ .

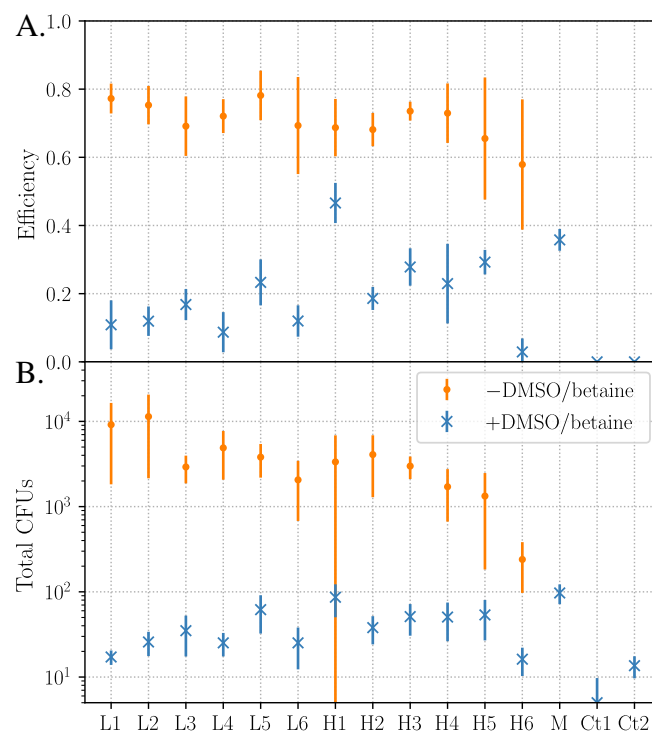


**Figure 2.** LCRs of a seven-part toy-plasmid by utilizing bridging oligo-sets (BO-sets) with high crosstalk (sets H1-H6) and low crosstalk (sets L1-L6). Each LCR was performed as a quintuplet. The standard deviation for each LCR is indicated by error bars. In addition to these twelve sets, a 13th set ("manual" set M) was utilized for the baseline-LCR (8%  $v/v$  DMSO and 0.45 M betaine). The total amount of colonies are plotted on a logarithmic scale. **A.** All LCRs without DMSO/betaine resulted in higher efficiencies in comparison to the LCRs with both detergents. No correlation between crosstalk and BO performance was found. Additionally, BO-set dependent differences were found for the baseline-LCRs, e.g., BO-set H1 resulted in a higher efficiency than BO-set L1. The negative control reactions with BOs without ligase (Ct1) and without BOs and ligase (Ct2) resulted in no fluorescent colonies. **B.** LCRs without DMSO/betaine resulted in more colonies in comparison to the baseline-conditions. The raw data of the LCRs presented here are shown in Supplementary Figure S1. The sequences of all BO-sets are shown in Supplementary Table S3. BO: bridging oligo, CFU: colony forming unit, DMSO: dimethyl sulfoxide.

An alternative approach to obtain higher assembly efficiencies without rising costs due to synthesizing longer oligonucleotides is to omit the liquids DMSO and betaine. This omission also aids automated liquid handling approaches because both detergents have unfavorable properties like extreme viscosities, hygroscopic characteristics and acting as surfactants. These new experimental conditions greatly improved both the efficiency and total number of CFUs (Figure 2). Consistent with the results of the LCRs with DMSO/betaine, the melting temperature is the most influencing parameter. As a result of the omission of DMSO and betaine, BO-sets with lower  $T_m$ s were favorable, yielding the greatest total amount of colonies at high efficiency

(Figure 3D). This behavior is also observed by comparing the total CFUs derived by utilizing the BO-sets L2, H1 and the manual one (Supplementary Figure S7). Similar to this seven-part toy-plasmid, another LCR-design with a  $T_m$ -independent BO-design (20 bp for each BO-half) was published by (11) where six parts in a range of 79 bp to 2061 bp were assembled with high efficiencies. The *Taq*-ligase and a two-step LCR-protocol with annealing and ligation at the same temperature of 60 °C were utilized.

An explanation for low efficiencies in the baseline-LCR is related to the large difference between the annealing temperature of 55 °C and ligation temperature of 66 °C in combination with the utilization of DMSO and betaine. Both detergents reduce the energies required for strand separations (29, 30). Together with the experimental temperatures, this may result in an extensive reduction of template for the ligase by separating already hybridized BO/probe double strands. Bridging oligo-sets with lower  $T_m$ s are theoretically more affected than sets with higher melting temperatures and should benefit from decreasing the temperature interval. Related to this, a reduction of the ligation temperature is expected to be advantageous. This was validated by using three BO-sets with different melting temperatures (Supplementary Figure S8) despite the ligation temperature of 60 °C being lower than the optimum temperature of the ligase (according to the manufacturer: 70 °C). Increasing the annealing temperature, which would also decrease the interval, was assumed to be disadvantageous due to accelerated BO/template-separation and was not investigated.

Several mechanisms are suspected to cause the total CFU decrease in LCRs with DMSO/betaine. First, lower LCR efficiencies result in fewer fully assembled plasmids and fewer colonies. The effects of DMSO and betaine were also investigated separately to prove these results (Supplementary Figure S9). Second, DMSO/betaine negatively influence the electroporation process. This can also be seen in Supplementary Figure S9, where an LCR without DMSO/betaine was mixed with both detergents before the electroporation and 3-4× fewer CFUs were obtained in comparison to DMSO/betaine-free controls. In contrast to the literature (8, 9), a lower volume-ratio of LCR and cells was used for the transformations (1:10; 2× higher concentration of DMSO/betaine). These conditions are not toxic for the *E. coli* strain NEB® 10-β because chemical transformations of the same strain with the plasmid pUC19 revealed no negative effects of utilizing a combination of DMSO and betaine (Supplementary Figure S12). A negative impact of DMSO and a positive impact of betaine was observed. A strain-dependent influence of DMSO in chemical transformations was described in (31) and such an influence is also plausible for betaine and a combination of both reagents. To counteract the CFU-reducing effects of detergents, a 30 min dialysis using *aq. dest.* and a nitrocellulose-membrane after the LCR was found to increase the amount of colonies (data not shown).

Performing LCRs without DMSO/betaine is recommended for the assembly of the seven fragments. To investigate optimal experimental temperatures for the new conditions without DMSO and betaine, the interaction of the annealing, ligation and BO-melting temperatures need to be considered.

### Increased annealing temperature is beneficial for LCRs without DMSO and betaine

To optimize the LCR without DMSO/betaine, several experiments were performed. Figure 3D shows that the BO-sets with low  $T_m$ s yield the most correct CFUs, which suggests that the BOs may bind too strongly to unwanted sites and be unavailable for ligation. To counteract this, the optimal annealing temperature was determined by performing a gradient-LCR, i.e. LCRs at different cycling conditions. For this, three new BO-sets were composed from the existing pool of BOs used in LCRs shown in Figure 2 to obtain sets with average melting temperatures of 67.8 °C, 69.9 °C and 71.8 °C (sequences in Supplementary Table S4). Within an annealing temperature range of 56.5 °C to 75.6 °C these sets were analyzed by chemically transforming the corresponding LCRs in chemically competent NEB® 10-β *E. coli*. This resulted in roughly 100× lower transformation efficiency in comparison to the electrocompetent cells utilized in previous experiments.

For all sets, the efficiency was similar throughout the entire temperature range (Figure 4A). Consistent with previous results, the total amount of CFUs increased with lower BO- $T_m$ s (comparing the results shown in Figures 3H and 4B). Furthermore, all sets have a global CFU maximum in the annealing temperature range of ~66-71 °C. This range contains the ligase optimum of 70 °C, which suggests positive effects of prolonging the total ligation time to 1.5 min (30 s annealing at 66-68 °C, 1 min ligation at 66 °C) in comparison to the baseline-condition of 30 s annealing at 55 °C and 1 min ligation at 66 °C.

In total, increasing the annealing temperature from 55 °C to 66 °C improved the CFU yield of every BO-set by a factor of two without a loss of efficiency. The BO-set "67.8 °C" performed better than the other sets. Supplementary Figure S11 shows that at the optimum annealing temperature of 67.8 °C, the BO-set "67.8 °C" also showed slightly greater efficiency than the other sets.

Lower BO melting temperatures may have additional benefits for LCR assemblies without DMSO and betaine. To validate this, new BO-sets with lower melting temperatures of 62 °C to 67.3 °C were designed and applied for ligations at 66 °C (Figure 4C+D, sequences in Supplementary Table S5). Surprisingly, a drop-off in efficiency and CFUs were observed for BO-sets with equal or lower melting temperatures than 66 °C. In comparison to the results shown in Figure 4A the efficiency of the 69.9 °C-set is 30% lower. This result is most likely related to a loss of function by additional freeze-thaw cycles or contamination of the DNA parts, BO-sets and/or supplements. Negative impacts of repeated freeze-thaw cycles on the DNA parts and BOs were already mentioned for the LCR (16) and for single-stranded oligonucleotides (32). Nevertheless, the total amount of CFUs was further optimized by increasing the annealing temperature in the range of the ligase optimum without decreasing the efficiency. Together with previous optimizations by performing the LCR without DMSO and betaine the assembly of the seven-part was highly improved.



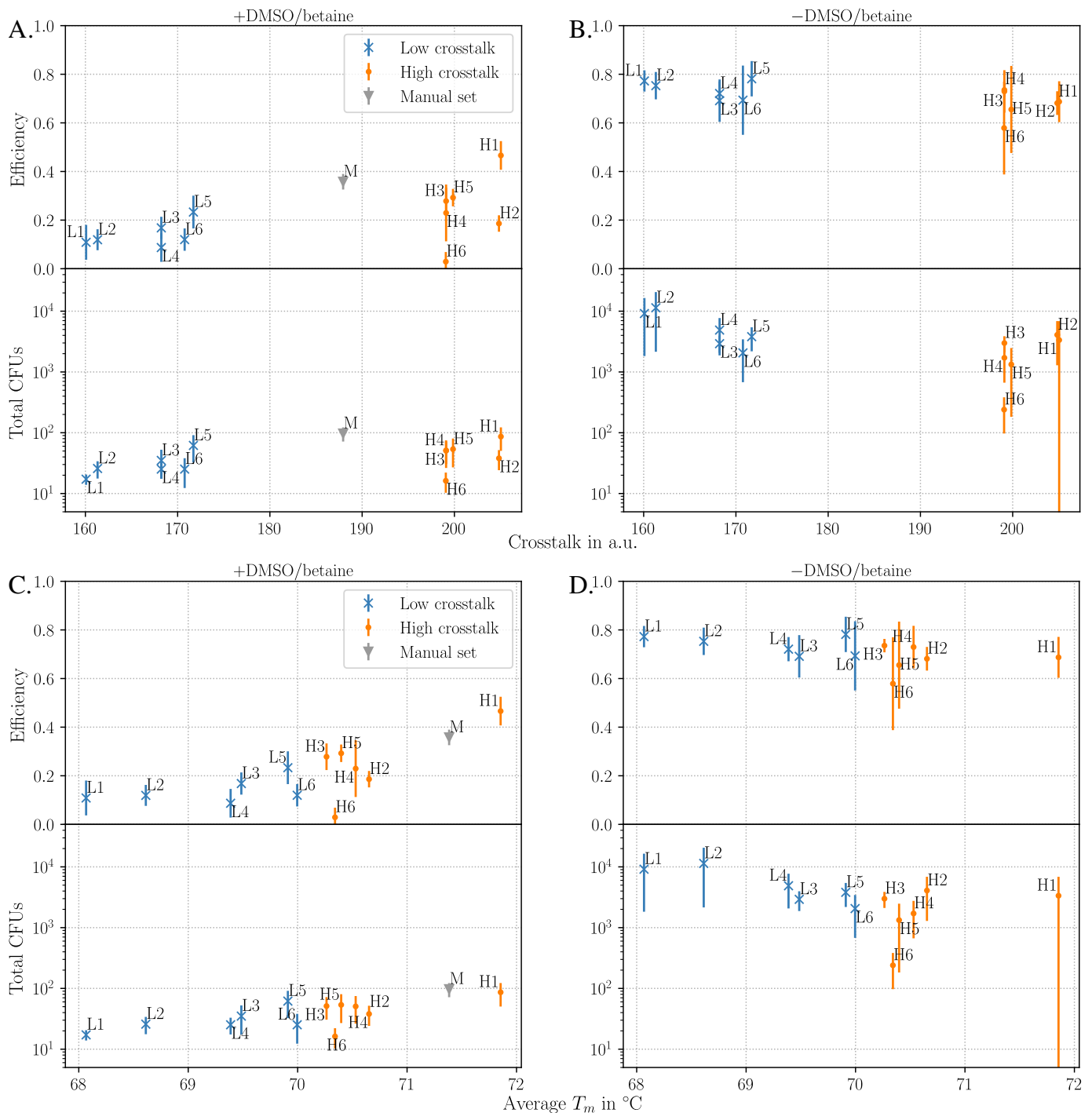


**Figure 3.** Graphical analysis of the bridging oligo sets (BO-sets) utilized for the assembly of a seven-part toy-plasmid, based on the results shown in Figure 2. The total colony forming units (CFUs) are plotted on a logarithmic scale. The standard deviation for each LCR is indicated by error bars. **A+B.** No crosstalk-dependent effects of the BOs were observed for the LCR with (A) and without (B) DMSO/betaine. Both clusters (L1-L6 and H1-H6) were distinguishable by the crosstalk but without affecting the LCR efficiency and total amount of colonies. Slightly higher efficiencies and more colonies were observed for the cluster of the sets H1-H6 when DMSO/betaine was used. **C+D.** The average melting temperature of the BO-sets influenced the LCRs. Higher  $T_m$ s resulted in higher efficiencies and more colonies when DMSO and betaine were used (C). Without DMSO and betaine, all BO-sets resulted in similar efficiencies suggesting no impact of crosstalk of BOs with the DNA parts in the LCR-assembly of the seven-part toy-plasmid. More colonies were observed for sets L1-L6. In contrast to LCRs with DMSO and betaine (C), the total amount of colonies was found to be increasing with decreasing melting temperatures. All  $T_m$ s presented here were calculated by using the formula of (20) for the  $T_m$  calculation and salt correction. The manual set ("M", used for LCRs with DMSO and betaine) was designed in Geneious with the same algorithms and a target temperature of 70 °C. The difference of  $\sim 1.5$  °C in comparison to the target  $T_m$  of 70 °C is due to the lack of an option to specify the DNA-part concentration in the software. The raw data of the LCRs presented here are shown in Supplementary Figure S1. a. u. arbitrary unit, BO: bridging oligo, CFU: colony forming unit, DMSO: dimethyl sulfoxide, M: manually designed BO-set,  $T_m$ : melting temperature of a BO-half.

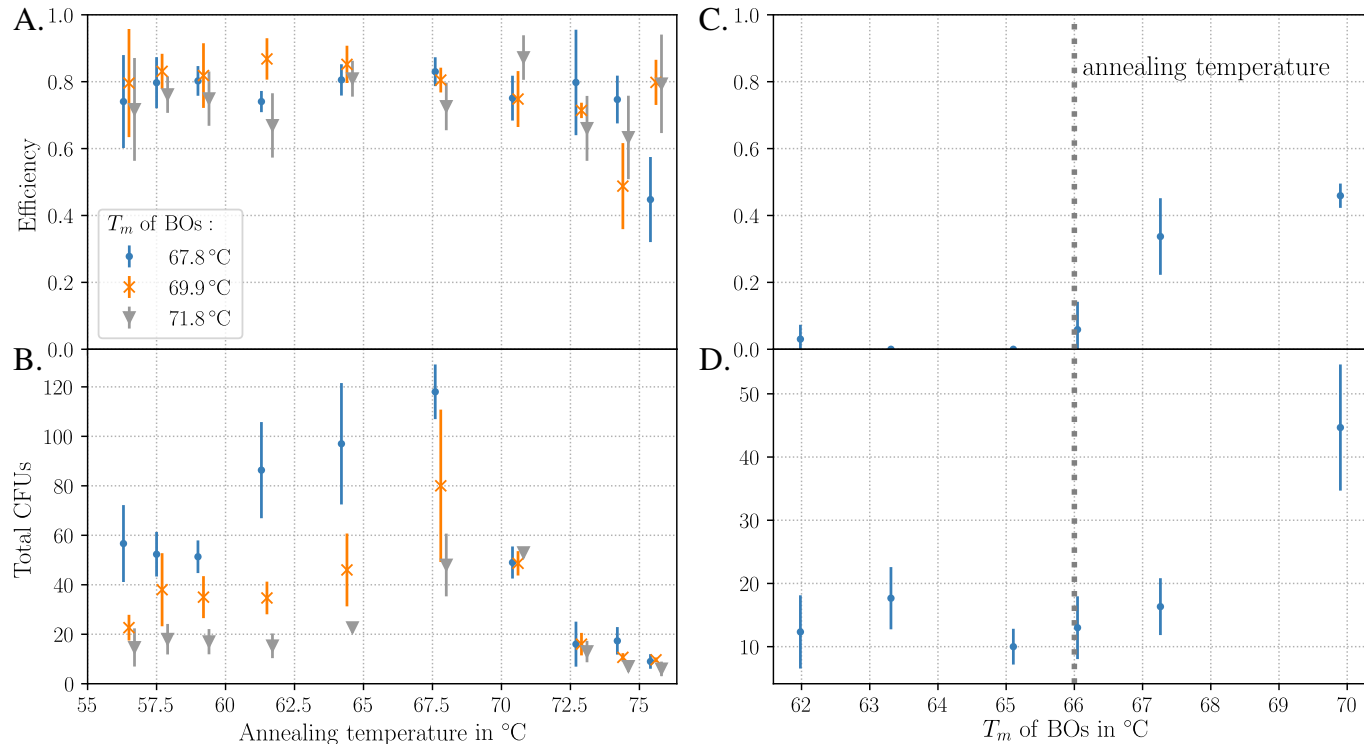


**Figure 4.** Adjustment of the annealing temperature and melting temperature of bridging oligo halves of DMSO/betaine-free LCR. The LCRs were performed as triplets using the same DNA-parts and chemically competent cells. The standard deviation for each LCR is indicated by error bars. **A.** For a better visibility the bars of the results were shifted with an offset of the annealing temperatures shown on the x-axis. Optimization of the annealing temperature of the seven-part plasmid via gradient-LCR. The temperature range for the annealing was 56.5 °C to 75.6 °C. Three BO-sets with different melting temperatures were used (67.8 °C, 69.9 °C and 71.8 °C). For the three BO-sets the LCR-efficiency was at a similar level. It started decreasing at an annealing temperature of more than 70.6 °C. **B.** As already observed in B (and Figure 3H), the total amount of colonies was increased with a lower BO- $T_m$ . Overall, the LCRs using these BO-sets resulted in a global maximum of colonies in a range of ~66-71 °C with 2× more colonies (also shown in Supplementary Figure S10). The BO-set sequences of the three sets are shown in Supplementary Table S4. **C+D.** Based on the optimization shown in A+B, the annealing temperature of 66 °C was used to investigate the influence of BO-halves with lower  $T_m$ s of 62.0 °C to 67.3 °C. As reference, the BO-set "71.8 °C" from A+B was used. Further decrease of the BO- $T_m$  did not improve the LCR at the optimized annealing temperature of 66 °C. In comparison to A the LCR with the BO-set "69.9 °C" was less efficient due to loss of function by repeated freeze-thaw cycles of the DNA parts and/or BOs. The sequences of the BO-sets "62.0 °C" to "67.3 °C" are shown in Supplementary Table S5. BO: bridging oligo, CFU: colony forming unit, DMSO: dimethyl sulfoxide,  $T_m$ : melting temperature of a BO-half.

### Optimizations are dependent on the size of DNA parts

In order to further validate the positive effects of omitting DMSO/betaine and to use a higher annealing temperature of 66 °C in DMSO/betaine free conditions, the sequence of the seven-part plasmid was used for a three-part split consisting of *mRFP1* as part 1, *sfGFP* as part 2 and pJET1.2/blunt as part 3. The BOs used for this assembly were externally resynthesized and new aliquots of all supplements. This plasmid was assembled by using the baseline and improved LCR conditions. For the baseline condition, the LCR was performed using the manual BO-set with a  $T_m$  of 71.4 °C for each half, 8% v/v DMSO, 0.45 M betaine and the annealing at 55 °C. For the improved LCR condition, the BO-set had a  $T_m$  of 67.8 °C for each half (set was already used for the gradient-LCR in Figure 4), no DMSO/betaine were used and the annealing was at 66 °C. The sequences of both BO-sets are shown in Supplementary Table S6. In general, the three-part plasmid was built by the two different LCR-protocols with no differences in the total plasmid size (4918 bp), sequence and BOs in comparison to the seven-part version.

Unexpectedly, the results for the three-part plasmid were contrary although the sequences and context remained the

same (Supplementary Figure S13). The use of DMSO/betaine and an annealing temperature of 55 °C are recommended and corroborate the literature (8, 9) but with a potential for further optimization. The efficiency was around 40%, similar to the assembly of the seven-part plasmid using the manual set (Figure 2A). As observed for LCRs with DMSO and betaine (Figure 3B), BOs with a higher  $T_m$  of 74.8 °C may improve the efficiency. Using 8% v/v DMSO and 0.45 M betaine has shown a positive impact for three-part plasmid, but proved detrimental for the seven-part plasmid that contains a very short part with 79 bp. To avoid higher costs for larger oligonucleotides, another approach for the optimization was to omit the  $T_m$ -decreasing substances DMSO and betaine. For the assembly of the seven-part plasmid, the efficiency and amount of colonies were highly increased (2-3× higher efficiency, Figure 2). The total amount of CFUs was further increased by adjusting the annealing temperature to 66 °C (Figure 4).

Besides general factors like the genetic context, total plasmid size, amount of parts, purification grade and freeze-thaw-cycles, the successful optimization of the LCR depends on the part size distribution. As hypothesized by de Kok et al.



(9), positive effects of DMSO/betaine utilization are related to accelerated strand separation during the denaturation step, so that the addition of both detergents should be advantageous for all LCR assemblies. However, the assembly of the seven-fragment plasmid showed a negative impact when adding both DMSO and betaine. Smaller subparts of a sequence denature faster into single strands than larger parts at the same thermodynamic conditions (33). A maximal denaturation of the DNA parts may be disadvantageous for the ligation, because BOs might anneal unspecifically to sites on completely single-stranded parts. A partially denatured DNA part might have single-stranded ends but a double-stranded central region, which is not available for unwanted BO hybridization. Assemblies of smaller parts are thus negatively affected by the utilization of DMSO and betaine whereas DMSO and betaine are necessary for larger parts to unwind the double-stranded ends for the annealing of the BO.

## CONCLUSION

To our knowledge, the presented assembly of a plasmid with *sfGFP* and *mRFP1* is the first documented experimental LCR-design that includes a direct and fast readout to investigate the influence of various plasmid designs and experimental conditions. The utilized toy-model plasmid in combination with the fluorescence-based analysis enables a robust and easy-to-adapt *in vivo* system to get valuable insights into the LCR and is also adaptable for investigations of other assembly techniques.

Based on this workflow, the impact of intramolecular and intermolecular crosstalk between BOs is assumed to be negligible for the assembly of the seven-part plasmid, whereas a strong sensitivity in regards to the BO  $T_m$  was observed. We revealed that a higher target- $T_m$  than 70 °C for the BO-design of LCRs utilizing DMSO and betaine is highly beneficial when compared with the published conditions. Related to this, it is of crucial importance to be consistent in the choice of the algorithms for the  $T_m$  calculation. Sets with a melting temperature of 74.8 °C when using the formula of SantaLucia (20) are recommended. A melting temperature of 72.2 °C is recommended when using the algorithms of SantaLucia (20) and the salt correction of Owcarzy et al. (28). Using guanosine or cytosine at the 3'-end of the BOs was not found to be necessary. If BO-sets with a target  $T_m$  of less than 70 °C are used, it is advantageous to decrease the ligation temperature from 66 °C to 60 °C.

For LCRs where smaller parts than 350 bp are included, the addition of 8% v/v DMSO and 0.45 M betaine is not necessary. Increasing the annealing temperature from 55 °C to 66 °C is useful for DMSO/betaine-free LCRs. To ensure high efficient assemblies, we provide an optimized step-by-step LCR-protocol for constructs with small parts (<350bp) and long parts (protocol in the supplement).

Altogether, these observations offer improved protocols for LCRs with and without 8% v/v DMSO and 0.45 M betaine to achieve highly efficient DNA assemblies. To further design more experimental rules for the LCR, the combination of *in vitro* studies using cell-free systems (34) and the toy-plasmid-based screening offers another approach to gain further insights of the LCR.

## ACKNOWLEDGEMENTS

We thank Carolin Dombrowsky for her technical support to perform the transformations of *E. coli* and the fluorescence-based screening. The authors also acknowledge the scientific discussions and advices with members of the "LOEWE CompuGene"-group. We further thank Brigitte Held and Dunja Sehn for their organizational support and Alexander Rapp for providing the fluorescence microscope and technical assistance.

## FUNDING

Hessen State Ministry of Higher Education, Research and the Arts (HMWK) via the LOEWE CompuGene project (to N.S., F.R., S.J., J.K.) and financial support of M.S. by the Deutsche Forschungsgemeinschaft within the GRK 1657, project 1A.

*Conflict of interest statement.* None declared.

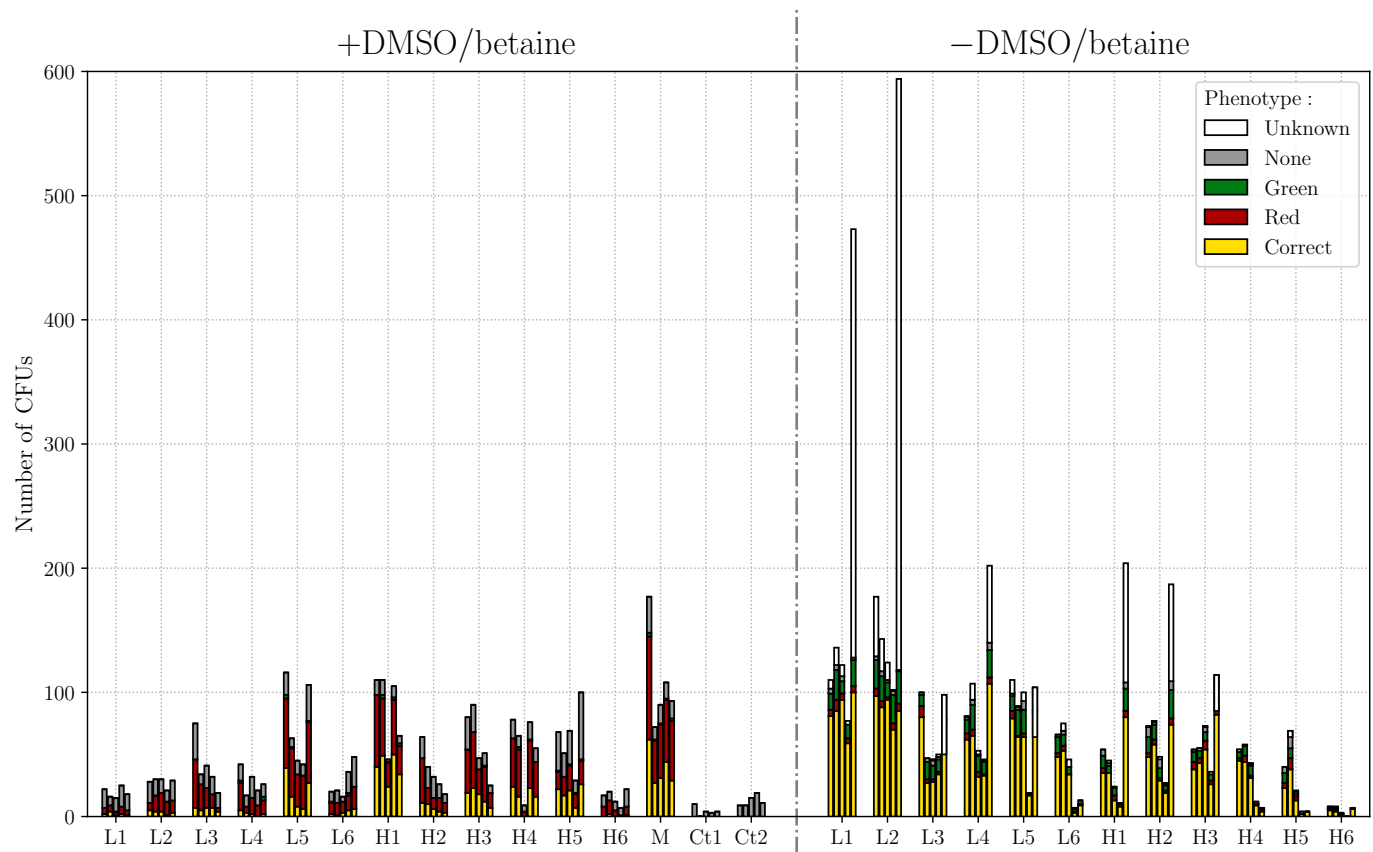
## SUPPLEMENTARY DATA

Supplementary data in pdf-file.

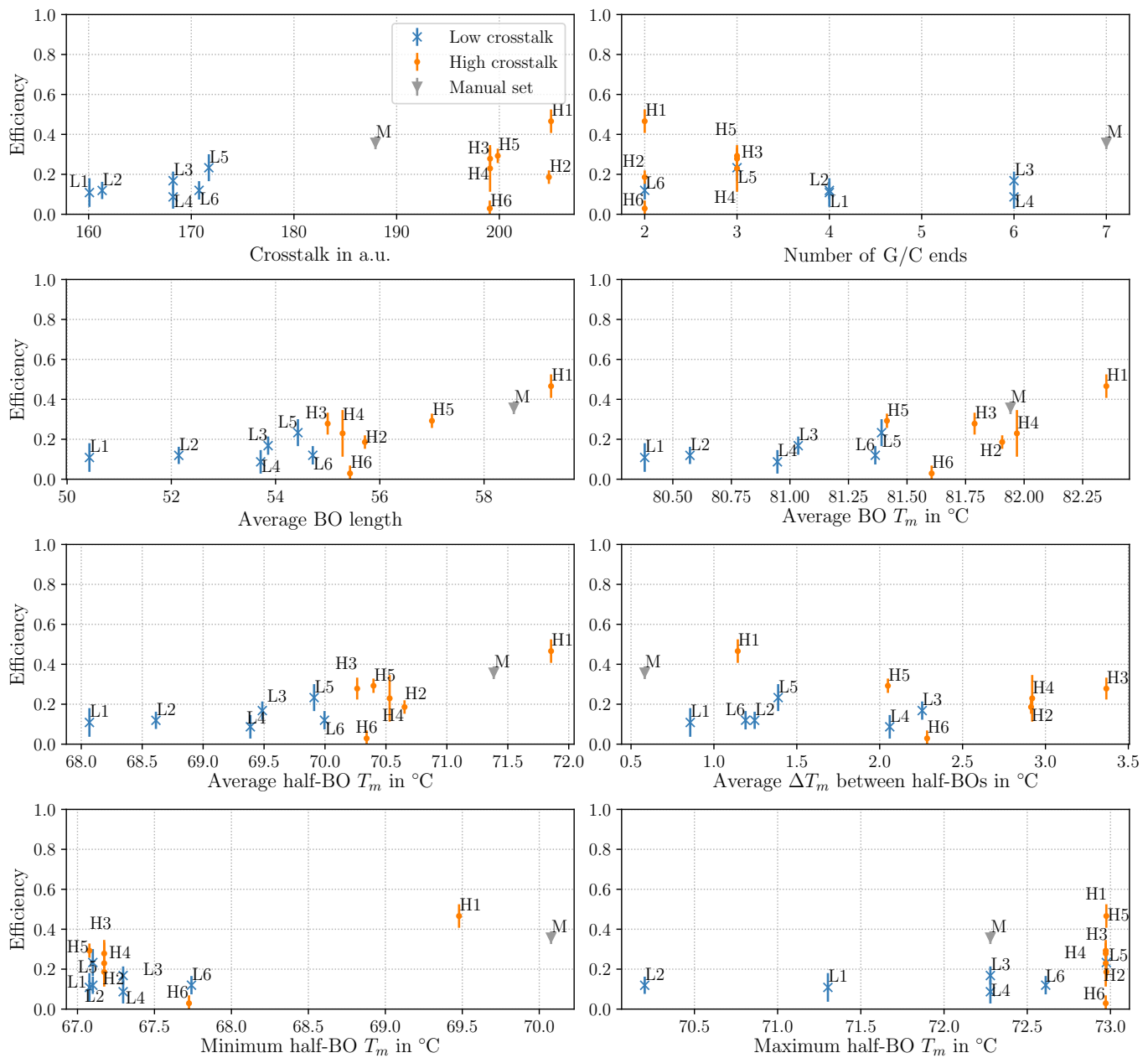
## REFERENCES

- Gibson,D.G., Young,L., Chuang,R.Y., Venter,J.C., Hutchison,C.A., and Smith,H.O. (May, 2009) Enzymatic assembly of DNA molecules up to several hundred kilobases. *Nature Methods*, **6**(5), 343–345.
- Engler,C., Kandzia,R., and Marillonnet,S. (November, 2008) A one pot, one step, precision cloning method with high throughput capability. *PLoS ONE*, **3**(11), e3647.
- Engler,C., Gruetzner,R., Kandzia,R., and Marillonnet,S. (May, 2009) Golden gate shuffling: a one-pot DNA shuffling method based on type II restriction enzymes. *PLoS ONE*, **4**(5), e5553.
- Quan,J. and Tian,J. (July, 2009) Circular polymerase extension cloning of complex gene libraries and pathways. *PLoS ONE*, **4**(7), e6441.
- Storch,M., Casini,A., Mackrow,B., Fleming,T., Trewitt,H., Ellis,T., and Baldwin,G.S. (July, 2015) BASIC: A new biopart assembly standard for idempotent cloning provides accurate, single-tier DNA assembly for synthetic biology. *ACS Synthetic Biology*, **4**(7), 781–787.
- Ma,H., Kunes,S., Schatz,P.J., and Botstein,D. (1987) Plasmid construction by homologous recombination in yeast. *Gene*, **58**(2), 201–216.
- Torella,J.P., Lienert,F., Boehm,C.R., Chen,J.H., Way,J.C., and Silver,P.A. (August, 2014) Unique nucleotide sequence-guided assembly of repetitive DNA parts for synthetic biology applications. *Nature Protocols*, **9**(9), 2075–2089.
- Chandran,S. (2017) Rapid assembly of DNA via ligase cycling Reaction (LCR). In Hughes,R.A., (ed.), *Synthetic DNA*, Vol. 1472, pp. 105–110 Springer New York New York, NY.
- de Kok,S., Stanton,L.H., Slaby,T., Durot,M., Holmes,V.F., Patel,K.G., Platt,D., Shapland,E.B., Serber,Z., Dean,J., Newman,J.D., and Chandran,S.S. (February, 2014) Rapid and reliable DNA assembly via ligase cycling reaction. *ACS Synthetic Biology*, **3**(2), 97–106.
- Pachuk,C.J., Samuel,M., Zurawski,J.A., Snyder,L., Phillips,P., and Satischandran,C. (February, 2000) Chain reaction cloning: a one-step method for directional ligation of multiple DNA fragments. *Gene*, **243**(1–2), 19–25.
- Roth,T.L., Milenkovic,L., and Scott,M.P. (September, 2014) A rapid and simple method for DNA engineering using cycled ligation assembly. *PLoS ONE*, **9**(9), e107329.
- Hendling,M., Pabinger,S., Peters,K., Wolff,N., Conzemius,R., and Barii,I. (July, 2018) Oli2go: an automated multiplex oligonucleotide design tool. *Nucleic Acids Research*, **46**(W1), W252–W256.
- SantaLucia,J. (2007) Physical principles and visual-OMP software for optimal PCR design. In Walker,J.M. and Yuryev,A., (eds.), *PCR Primer Design*, Vol. 402, pp. 3–33 Humana Press Totowa, NJ.
- Nowak,R.M., Wojtowicz-Krawiec,A., and Plucienniczak,A. (2015) DNASynth: a computer program for assembly of artificial gene parts in decreasing temperature. *BioMed Research International*, **2015**, 1–8.
- Bode,M., Khor,S., Ye,H., Li,M.H., and Ying,J.Y. (July, 2009) TmPrime: fast, flexible oligonucleotide design software for gene synthesis. *Nucleic Acids Research*, **37**(suppl\_2), W214–W221.
- Robinson,C.J., Dunstan,M.S., Swainston,N., Titchmarsh,J., Takano,E., Scrutton,N.S., and Jervis,A.J. (January, 2018) Chapter Thirteen - Multifragment DNA Assembly of Biochemical Pathways via Automated Ligase Cycling Reaction. In Scrutton,N., (ed.), *Methods in Enzymology*, Vol. 608 of Enzymes in synthetic biology, pp. 369–392 Academic Press.
- Lee,M.E., DeLoache,W.C., Cervantes,B., and Dueber,J.E. (September, 2015) A highly characterized yeast toolkit for modular, multipart assembly. *ACS Synthetic Biology*, **4**(9), 975–986.
- Kearse,M., Moir,R., Wilson,A., Stones-Havas,S., Cheung,M., Sturrock,S., Buxton,S., Cooper,A., Markowitz,S., Duran,C., Thierer,T., Ashton,B., Meintjes,P., and Drummond,A. (June, 2012) Geneious basic: an integrated and extendable desktop software platform for the organization and analysis of sequence data. *Bioinformatics*, **28**(12), 1647–1649.
- Untergasser,A., Cutcutache,I., Koressaar,T., Ye,J., Faircloth,B.C., Remm,M., and Rozen,S.G. (August, 2012) Primer3-new capabilities and interfaces. *Nucleic Acids Research*, **40**(15), e115.
- SantaLucia,J. (February, 1998) A unified view of polymer, dumbbell, and oligonucleotide DNA nearest-neighbor thermodynamics. *Proceedings of the National Academy of Sciences*, **95**(4), 1460–1465.
- von Ahsen,N., Wittwer,C.T., and Schütz,E. (2001) Oligonucleotide melting temperatures under PCR conditions: nearest-neighbor corrections for Mg<sup>2+</sup>, deoxynucleotide triphosphate, and dimethyl sulfoxide concentrations with comparison to alternative empirical formulas. *Clinical Chemistry*, **47**(11), 1956–1961.
- Zhang,Y., Werling,U., and Edlmann,W. (April, 2012) SLiCE: a novel bacterial cell extract-based DNA cloning method. *Nucleic Acids Research*, **40**(8), e55.
- Jacobus,A.P. and Gross,J. (March, 2015) Optimal cloning of PCR fragments by homologous recombination in *Escherichia coli*. *PLoS ONE*, **10**(3), e0119221.
- Bzymek,M. and Lovett,S.T. (July, 2001) Instability of repetitive DNA sequences: the role of replication in multiple mechanisms. *Proceedings of the National Academy of Sciences*, **98**(15), 8319–8325.
- Dutra,B.E., Sutura,V.A., and Lovett,S.T. (January, 2007) RecA-independent recombination is efficient but limited by exonucleases. *Proceedings of the National Academy of Sciences*, **104**(1), 216–221.
- Geissmann,Q. (February, 2013) OpenCFU, a new free and open-source software to count cell colonies and other circular objects. *PLoS ONE*, **8**(2), e54072.
- Carpenter,A.E., Jones,T.R., Lamprecht,M.R., Clarke,C., Kang,I.H., Friman,O., Guertin,D.A., Chang,J.H., Lindquist,R.A., Moffat,J., Golland,P., and Sabatini,D.M. (October, 2006) CellProfiler: image analysis software for identifying and quantifying cell phenotypes. *Genome Biology*, **7**(10), R100.
- Owczarzy,R., Moreira,B.G., You,Y., Behlke,M.A., and Walder,J.A. (May, 2008) Predicting stability of DNA duplexes in solutions containing magnesium and monovalent cations. *Biochemistry*, **47**(19), 5336–5353.
- Escara,J.F. and Hutton,J.R. (July, 1980) Thermal stability and renaturation of DNA in dimethyl sulfoxide solutions: acceleration of the renaturation rate. *Biopolymers*, **19**(7), 1315–1327.
- Henke,W., Herdel,K., Jung,K., Schnorr,D., and Loening,S.A. (October, 1997) Betaine improves the PCR amplification of GC-rich DNA sequences. *Nucleic Acids Research*, **25**(19), 3957–3958.
- Hanahan,D. (June, 1983) Studies on transformation of *Escherichia coli* with plasmids. *Journal of Molecular Biology*, **166**(4), 557–580.
- Davis,D.L., O’Brie,E.P., and Bentzley,C.M. (October, 2000) Analysis of the degradation of oligonucleotide strands during the freezing/thawing processes using MALDI-MS. *Analytical Chemistry*, **72**(20), 5092–5096.
- Dwight,Z., Palais,R., and Wittwer,C.T. (April, 2011) uMELT: prediction of high-resolution melting curves and dynamic melting profiles of PCR products in a rich web application. *Bioinformatics*, **27**(7), 1019–1020.
- Shin,J. and Noireaux,V. (January, 2012) An *E. coli* cell-free expression toolbox: application to synthetic gene circuits and artificial cells. *ACS Synthetic Biology*, **1**(1), 29–41.

SUPPLEMENT

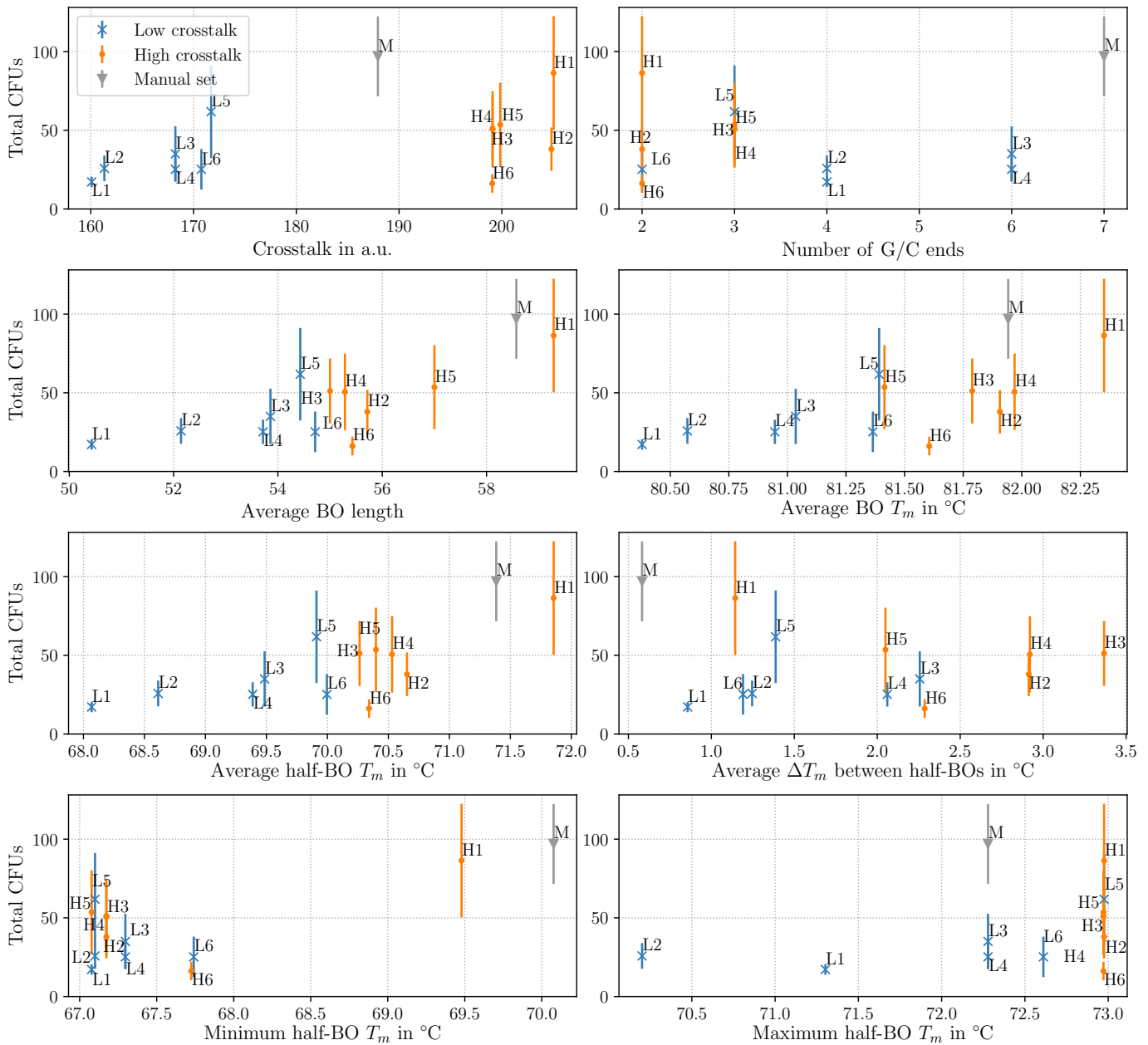


**Supplementary Figure S1.** Overview of raw data of the experiments to investigate and calculate the influence/omission of DMSO and betaine of the seven-part toy-plasmid (Figures 2 and 3). All LCRs were performed as quintuplets. The standard deviation for each LCR is indicated by error bars. Bridging oligo sets with minimized (L1-L6) crosstalk, maximized (H1-H6) crosstalk and the manually designed set (M) are presented. The negative control reactions with BOs without ligase (Ct1) and without BOs and ligase (Ct2) resulted in no fluorescent colonies and were only performed for the LCRs with DMSO/betaine. For the LCRs without DMSO and betaine the amount of CFUs presented here were corrected by multiplying them with the correction factor of 50. All CFUs were counted, but only the phenotypes of about 100 CFUs per LCR were determined. White bars indicate CFUs where the phenotype was not determined. 100 CFUs per LCR. All BO sequences are shown in Supplementary Table S3. BO: bridging oligo, CFU: colony forming unit, DMSO: dimethyl sulfoxide,  $T_m$ : melting temperature of a BO-half.

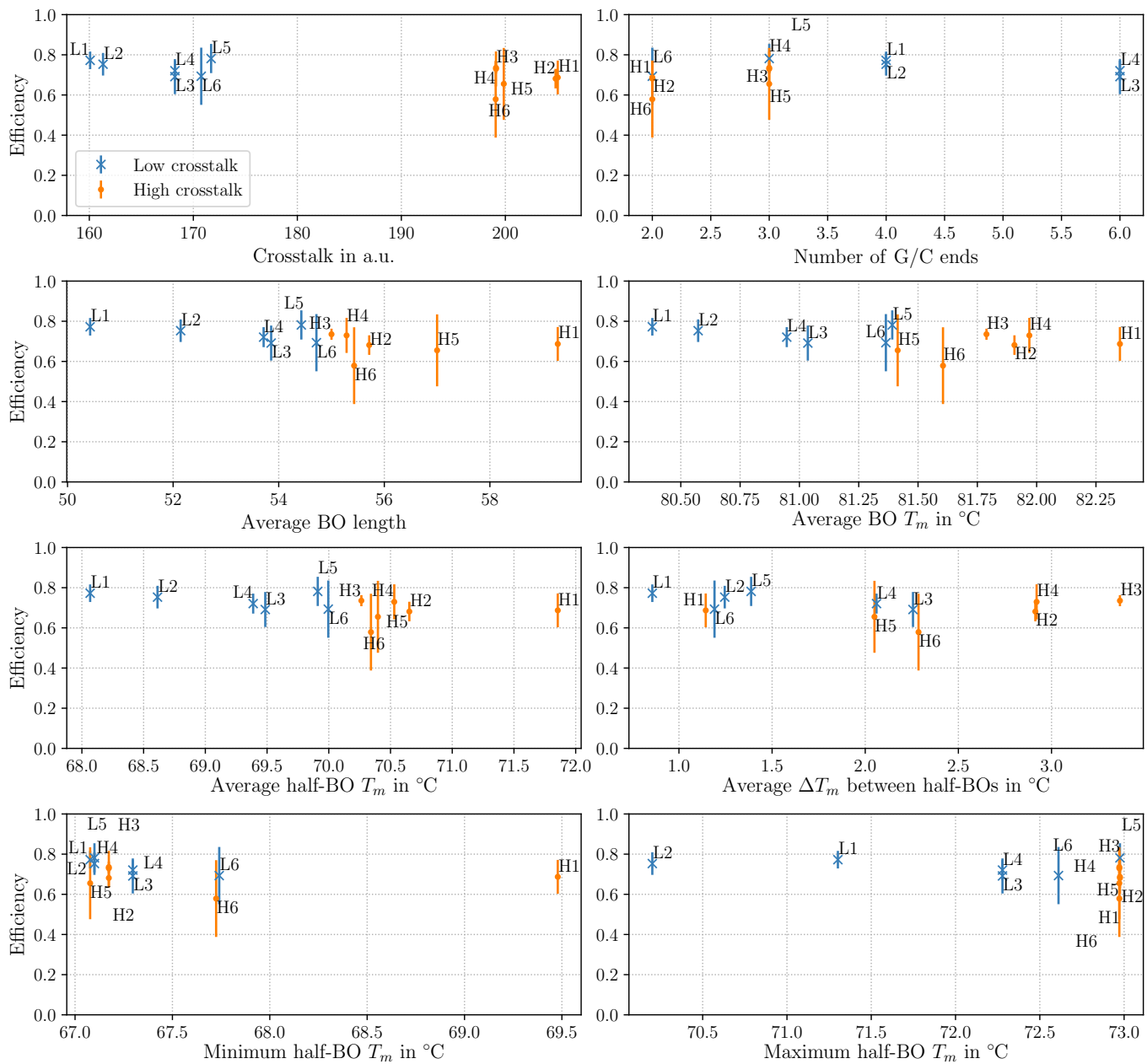


**Supplementary Figure S2.** Graphical analysis of LCRs with 8%  $v/v$  DMSO and 0.45 M betaine of the seven-part toy-plasmid and the influence of various predictors on the efficiencies by utilizing different bridging oligo sets. All LCRs were performed as quintuplets. The standard deviation for each LCR is indicated by error bars. All BO sequences are shown in Supplementary Table S3. a. u.: arbitrary unit, BO: bridging oligo, DMSO: dimethyl sulfoxide, G/C end: 3'-end of one BO ending with the nucleobase guanine or cytosine,  $T_m$ : melting temperature.

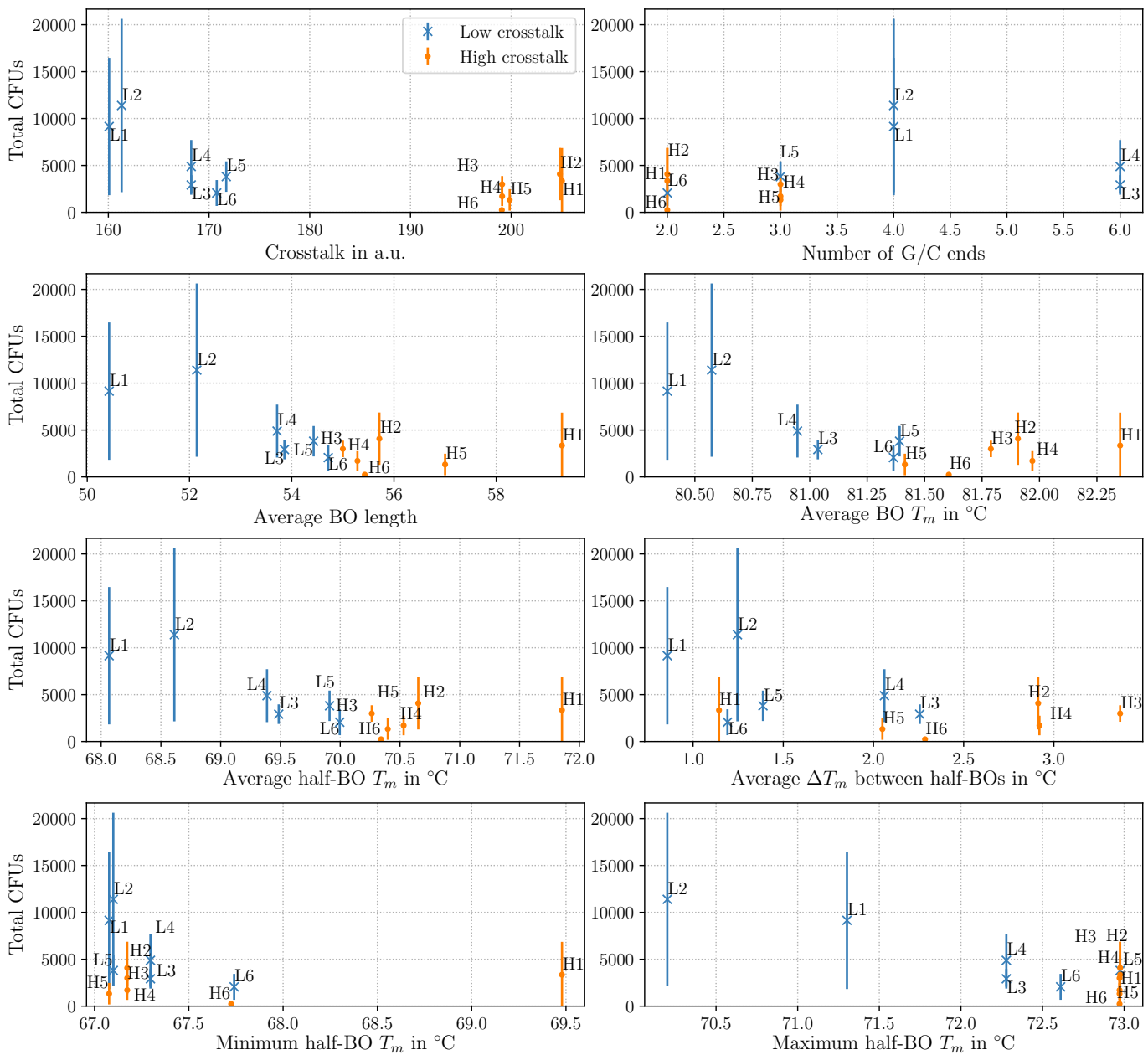




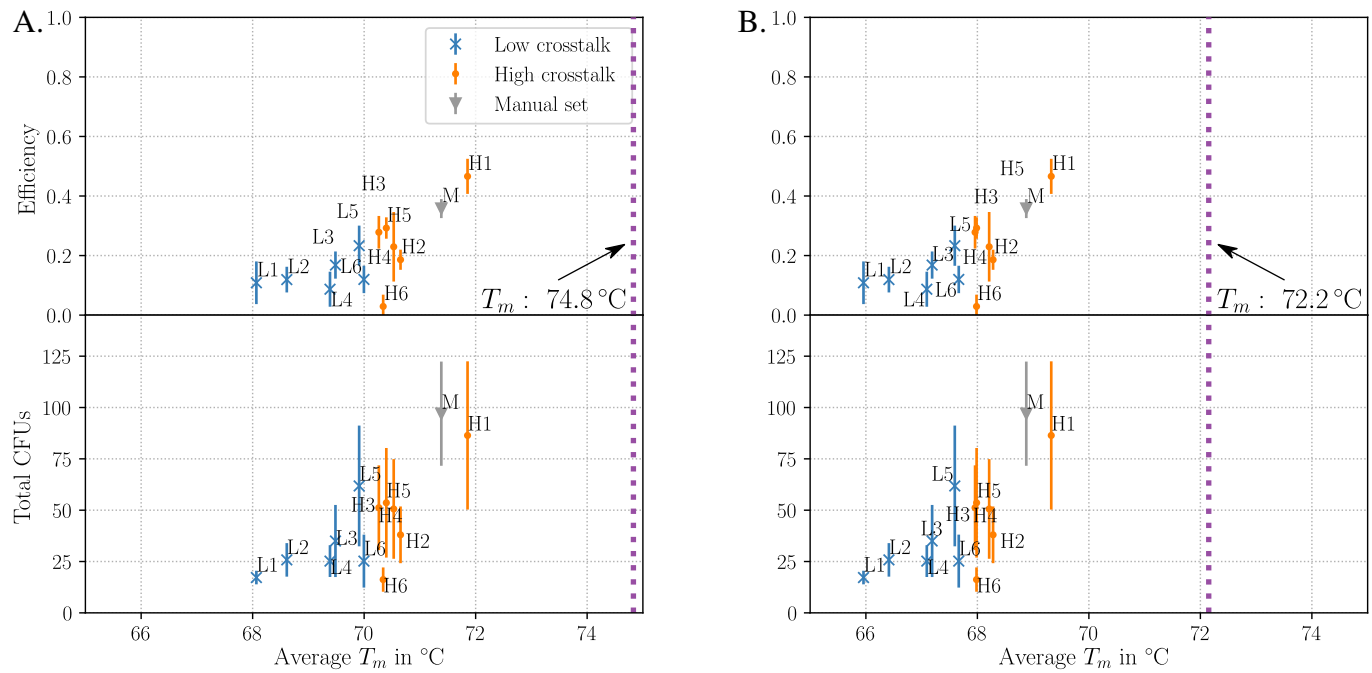
**Supplementary Figure S3.** Graphical analysis of LCRs with 8% v/v DMSO and 0.45 M betaine of the seven-part toy-plasmid and the influence of various predictors on the total amount of colonies by utilizing different bridging oligo sets. All LCRs were performed as quintuplets. The standard deviation for each LCR is indicated by error bars. All BO sequences are shown in Supplementary Table S3. a. u.: arbitrary unit, BO: bridging oligo, CFU: colony forming unit, DMSO: dimethyl sulfoxide, G/C end: 3'-end of one BO ending with the nucleobase guanine or cytosine,  $T_m$ : melting temperature.



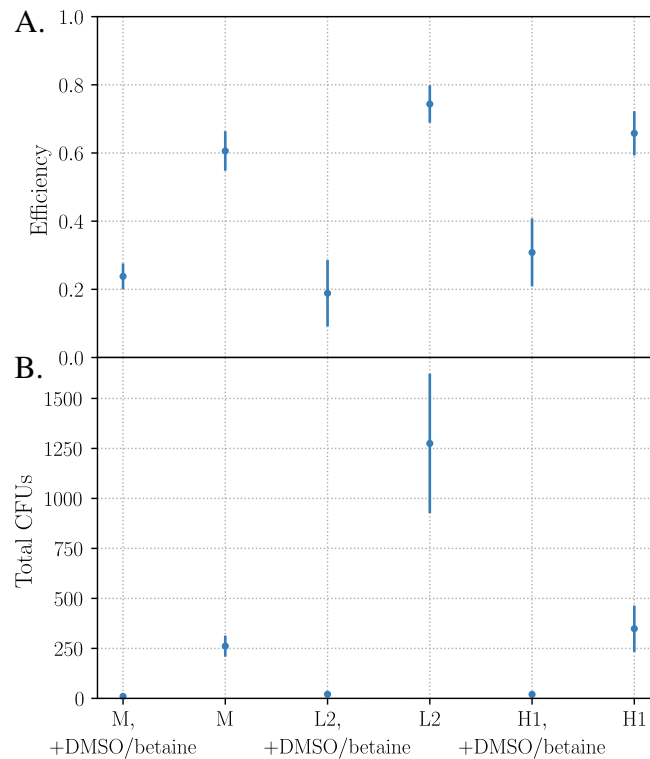
**Supplementary Figure S4.** Graphical analysis of LCRs without 8%  $v/v$  DMSO and 0.45 M betaine of the seven-part toy-plasmid and the influence of various predictors on the efficiencies by utilizing different bridging oligo sets. All LCRs were performed as quintuplets. The standard deviation for each LCR is indicated by error bars. All BO sequences are shown in Supplementary Table S3. a. u.: arbitrary unit, BO: bridging oligo, DMSO: dimethyl sulfoxide, G/C end: 3'-end of one BO ending with the nucleobase guanine or cytosine,  $T_m$ : melting temperature.



**Supplementary Figure S5.** Graphical analysis of LCRs without 8% v/v DMSO and 0.45 M betaine of the seven-part toy-plasmid and the influence of various predictors on the total amount of colonies by utilizing different bridging oligo sets. All LCRs were performed as quintuplets. The standard deviation for each LCR is indicated by error bars. All BO sequences are shown in Supplementary Table S3. a. u.: arbitrary unit, BO: bridging oligo, CFU: colony forming unit, DMSO: dimethyl sulfoxide, G/C end: 3'-end of one BO ending with the nucleobase guanine or cytosine,  $T_m$ : melting temperature.

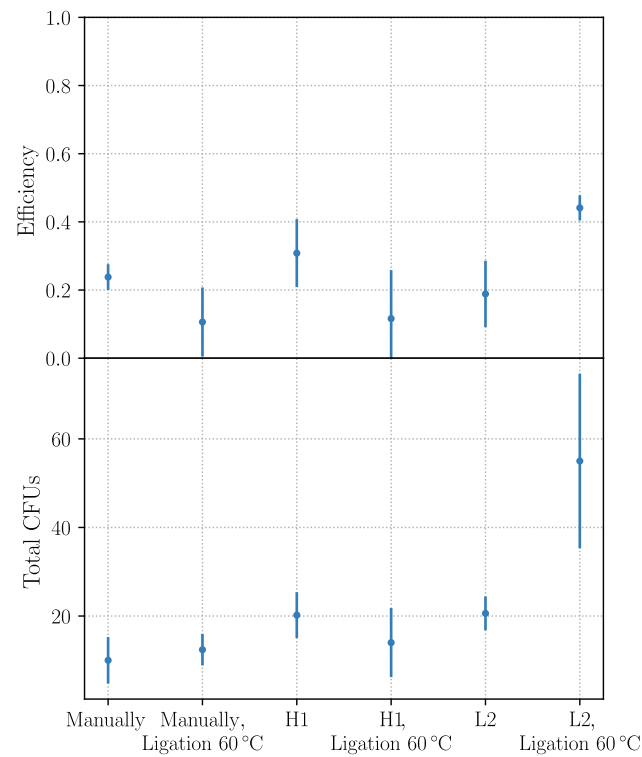


**Supplementary Figure S6.** Effect of salt corrections on melting temperature. The results for the LCRs with 8%  $v/v$  DMSO and 0.45 M are presented here. The thermodynamic parameters used were SantaLucia (20). The standard deviation for each LCR is indicated by error bars. **A.** SantaLucia (20) salt correction. **B.** Owczarzy (28) salt correction. The optimized melting temperature indicated by the dotted line is obtained from recalculation of the optimized BO-set of the de Kok et al. (9) study. BO: bridging oligo, CFU: colony forming unit, DMSO: dimethyl sulfoxide,  $T_m$ : melting temperature of one BO-half.

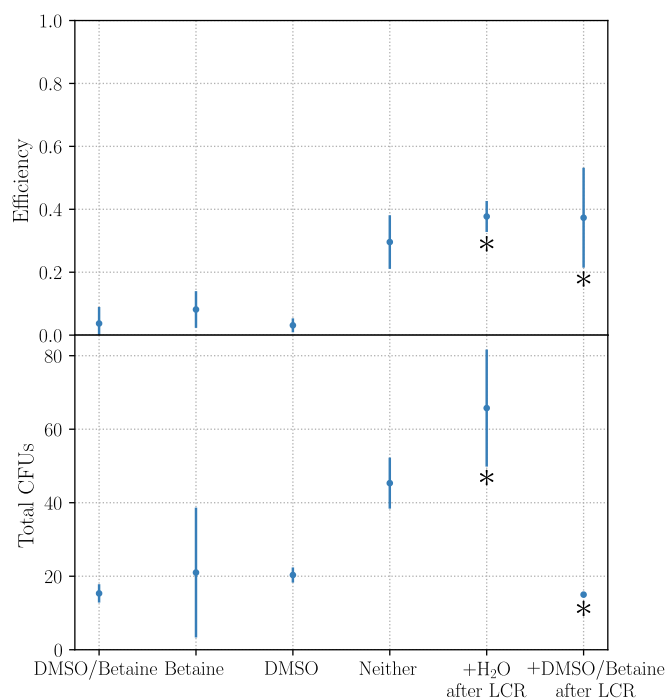


**Supplementary Figure S7.** Influence of DMSO and betaine in the LCR. All LCRs were performed as quintuplets using the same batches of DNA parts, electrocompetent cells and a master-mix (excluding the BO-sets and the ligase). The standard deviation for each LCR is indicated by error bars. **A.** For all three BO-sets (H1, L2 and the manually set) the DMSO/betaine-free LCRs were more efficient. As observed in Figure 2, the efficiency of the set "H1" was higher than the manual set "M" and set "L2" in the baseline-LCR (with DMSO and betaine). **B.** The omission of DMSO/betaine highly increased the total amount of colonies. This is consistent with the results shown in Figure 2B and 3H for DMSO/betaine-free conditions: a lower  $T_m$  is beneficial and resulted in more colonies. All BO sequences are shown in Supplementary Table S3.

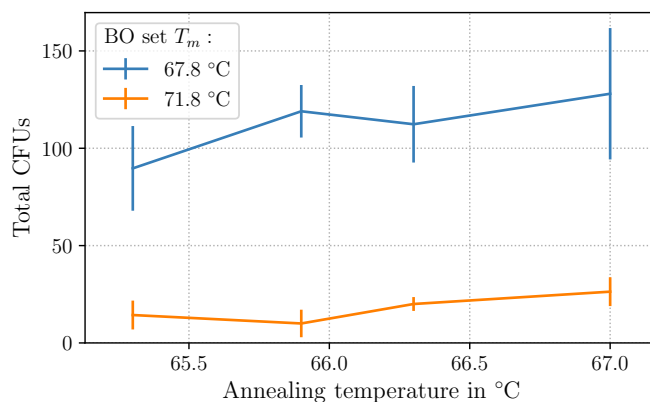




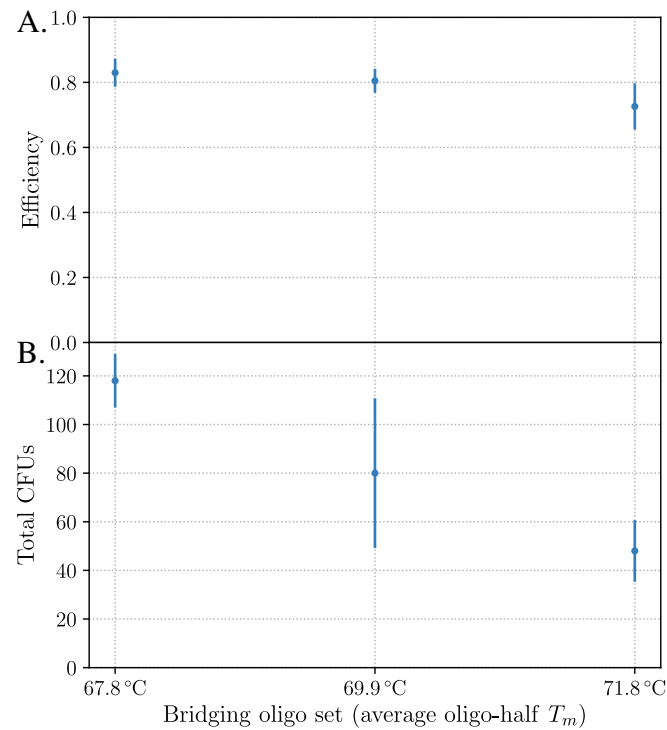
**Supplementary Figure S8.** Impact of the ligation temperature on LCR performance with DMSO and betaine. All LCRs were performed as quintuplets. The standard deviation for each LCR is indicated by error bars. A lower ligation temperature is beneficial for the efficiencies and total amount of colonies for the LCR using BO-set L2. This set had a lower  $T_m$  of 68.6 °C compared to the manual set with a  $T_m$  of 71.4 °C and the set H1 with a  $T_m$  of 71.9 °C. Due to the lowered ligation temperature, more BOs of set L2 remained attached to the DNA parts to guide the ligase. All BO sequences are shown in Supplementary Table S3.



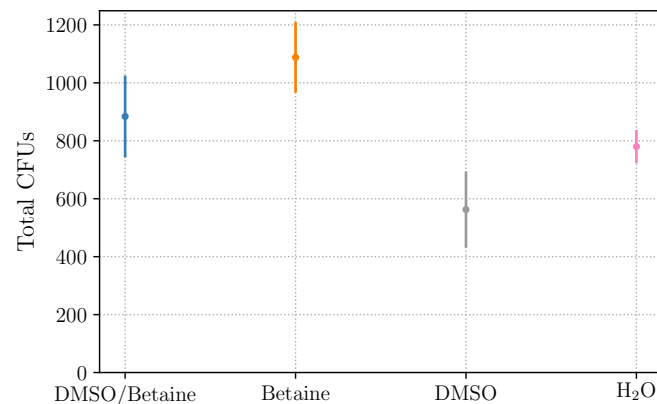
**Supplementary Figure S9.** DMSO and betaine negatively affect the LCR of the seven-part plasmid. The LCRs to investigate the impact of DMSO and/or betaine were performed as triplicates. To investigate the direct influence of DMSO and betaine on the electroporation process, the LCRs were performed as quadruplets (indicated with a \*). The standard deviation for each LCR is indicated by error bars and the manual set "M" was used. The combination of DMSO and betaine negatively affects the efficiency and the total amount of colonies (comparing the results for DMSO/betaine with none of both). Further investigation revealed a direct negative impact of DMSO/betaine in the electroporation. An LCR was performed without DMSO/betaine. Both detergents were added before the electroporation to simulate the transformation conditions (8% v/v DMSO and 0.45 M betaine, mix of 3  $\mu$ L LCR and 30  $\mu$ L competent cells). As a control *ddH*<sub>2</sub>O was added. All BO sequences are shown in Supplementary Table S3. BO: bridging oligo, CFU: colony forming unit, DMSO: dimethyl sulfoxide.



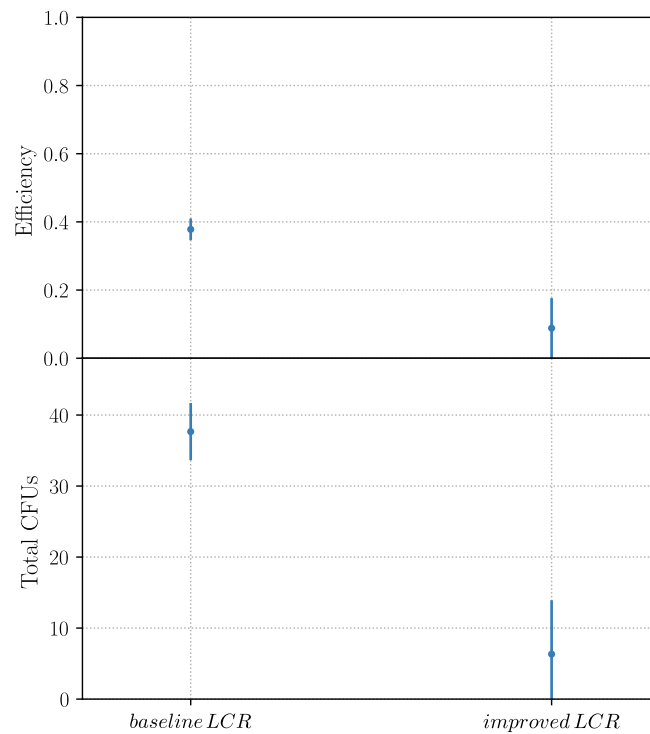
**Supplementary Figure S10.** Total amount of colonies for the bridging oligo sets "67.8 °C" and "71.8 °C" in the annealing temperature range of 65-67 °C (larger temperature range shown in Figure 4A+B). All LCRs were performed as triplets. The standard deviation for each LCR is indicated by error bars. All BO sequences are shown in Supplementary Table S4. BO: bridging oligo, CFU: colony forming unit, DMSO: dimethyl sulfoxide,  $T_m$ : melting temperature of one BO-half.



**Supplementary Figure S11.** LCR without DMSO and betaine at the annealing temperature of 67.9 °C using three bridging oligo sets ( $T_m = 67.8, 69.9$  and 71.8 °C). All LCRs were performed as triplets. The standard deviation for each LCR is indicated by error bars. A larger range of the annealing temperature is shown in Figure 4A+B. **A.** The efficiencies of the LCRs were similar. **B.** The total amount of colonies increased with lower melting temperatures of the BOs. All BO sequences are shown in Supplementary Table S4. BO: bridging oligo, CFU: colony forming unit, DMSO: dimethyl sulfoxide,  $T_m$ : melting temperature of one BO-half.



**Supplementary Figure S12.** DMSO and betaine in chemical transformations. All transformations were performed as triplets. The standard deviation for each LCR is indicated by error bars. The plasmid pUC19 was mixed with DMSO and/or betaine or *aq. dest.* followed by chemical transformation of *E. coli*. DMSO had a negative impact whereas betaine had a positive impact on the number of colonies. Adding both yielded similar results as adding neither. CFU: colony forming unit, DMSO: dimethyl sulfoxide.



**Supplementary Figure S13.** Improved and baseline LCR conditions of the three-part toy-plasmid. In contrast to the seven-part split of the same plasmid, the LCR with 8% v/v DMSO, 0.45 M, a BO-set with a  $T_m$  of 71.4 °C and an annealing at 55 °C resulted in a higher efficiency and more CFUs ("baseline LCR"). The improved conditions were without DMSO/betaine, a BO-set with a  $T_m$  of 67.9 °C and an annealing at 66 °C ("improved LCR"). All LCRs were performed as triplets. The BO sequences are shown in Supplementary Table S6. BO: bridging oligo, CFU: colony forming unit, DMSO: dimethyl sulfoxide,  $T_m$ : melting temperature of one BO-half.



## Toy-model plasmid

Supplementary Table S1: Sequences of the toy-model parts (Figure 1B). The bridging oligos were designed by concatenating subsequences of these parts. It was not necessary to use the reverse complement for the design because the experiments contained both strands of these parts. *mRFP1*: monomeric red fluorescent protein 1, *sfGFP*: superfolder green fluorescent protein.

Toy-Plasmid Part	Part Size (bp)	Sequence (5'→3')
<i>mRFP1</i> (Addgene: pYTK090)		
part 1 ( <i>mRFP1</i> -part 1)	79	TCCCTATCAGTGATAGAGATTGACATCCCTATCAGTGATAGAGATACTGAGCACGGATCTGA-AAGAGGAGAAAGGATCT
part 2 ( <i>mRFP1</i> -part 2)	330	ATGGCGAGTAGCGAAGACGTTATCAAAGAGTTCATGCGTTTCAAAGTTCGTATGGAAGGTTCCGTTAACGGTCACGAGTTCGAAATCGAAGGTGAAGGTGAAGGTCGTCCTGACGAAAGGTTACT-CAGACCGCTAAACTGAAAGTTACCAAAGGTGGTCCGCTGCCGTTTCGCTTGGGACATCCTGTC-CCCGCAGTTCAGTACGGTTCGAAAGCTTACGTTAAACACCCGGCTGACATCCCGGACTACCTGAAACTGTCTTCCCGGAAGGTTTCAAATGGGAACGTGTTATGAACTTCGAAGACGGTGGT-GTTGTTACCGTTACCCAGGAC
part 3 ( <i>mRFP1</i> -part 3)	523	TCCTCCCTGCAAGACGGTGAAGTTCATCTACAAAGTAAACTGCGTGGTACTAACTTCCCCTGTC-CGACGGTCCGGTTATGCAGAAAAAACCATGGGTTGGGAAGCTTCCACCGAACGTATGTAC-CCGGAAGACGGTGTCTGAAAGGTGAAATCAAATGCGTCTGAAACTGAAAGACGGTGGTCT-ACTACGACGCTGAAGTAAAACCACTACATGGCTAAAAACCGGTTACGCTGCCGGGTGC-TTACAAAACCGACATCAAAGTGGACATCACCTCCCAACGAAGACTACACCATCGTTGAA-CAGTACGAACGTGCTGAAGGTGCTCACTCCACCGGTGCTTAATAAGGATCTCCAGGCATCAA-ATAAAACGAAAGGCTCAGTCGAAAGACTGGGCCTTTCGTTTTATCTGTTGTTTGTCCGGTGAA-CGCTCTCTACTAGAGTCACACTGGCTCACCTTCGGGTGGGCCTTTCGCTTTTATAAGTCGGT-CTCACCGAGCGGCCGCTGTTACAACCAAT
<i>sfGFP</i> (Addgene: pYTK001)		
part 4 ( <i>sfGFP</i> -part 1)	305	GAAAGTGAAACGTGATTTTCATGCGTCATTTTGAACATTTTGTAAATCTTATTTAATAATGTGT-GCGGCAATTCACATTTAATTTATGAATGTTTTCTTAACATCGCGCAACTCAAGAAACGGCA-GGTTCCGGATCTTAGCTACTAGAGAAAAGAGGAGAAATACTAGATGCGTAAAGGCGAAGAGCT-GTTCACTGGTGTGCTCCCTATTCTGGTGGAACTGGATGGTGTGTAACGGTCATAAGTTTTTC-CGTGCGTGGCGAGGGTGAAGGTGACGCAACTAATGGTAAACTGACGCTGAAAGTTCA
part 5 ( <i>sfGFP</i> -part 2)	306	TCTGTACTACTGGTAACTGCCGGTTCCTTGGCCGACTCTGGTAAACGACGCTGACTTATGGT-GTTTCAGTGTCTTGGCTCGTTATCCGGACCATATGAAGCAGCATGACTTCTTCAAGTCCGCCAT-GCCGGAAGGCTATGTGCAGGAACGCACGATTTCTTTAAGGATGACGGCACGTACAAAACG-CGTGCGGAAGTGAAATTTGAAGGCGATACCCTGGTAAACCGCATTGAGCTGAAAGGCATTG-ACTTTAAAGAGGACGGCAATATCCTGGGCCATAAGCTGGAATACAATTTTAAACAGCCACA
part 6 ( <i>sfGFP</i> -part 3)	401	ATGTTTACATCACCGCCGATAAAACAAAAAATGGCATTAAAGCGAATTTTAAATTCGCCAC-AACGTGGAGGATGGCAGCGTGCAGCTGGCTGATCACTACCAGCAAAACACTCCAATCGGTG-ATGGTCTGTCTGCTGCCAGACAATCACTATCTGAGCACGAAAGCGTTCGTCTAAAGAT-CCGAACGAGAAACCGCATCATATGGTTCTGCTGGAGTTCGTAACCCGACGGGCATCACGC-ATGGTATGGATGAACTGTACAAATGACCAGGCATCAAATAAAACGAAAGGCTCAGTCGAAA-GACTGGGCCTTTCGTTTTATCTGTTGTTTGTCCGGTGAACGCTCTACTAGAGTCACACTGGC-TCACCTTCGGGTGGGCCTTTCGCTTTATA

Supplementary Table S1: Sequences of the toy-model parts (continued)

Toy-Plasmid Part	Part Size (bp)	Sequence (5'→3')
part 7 (pJET1.2/blunt)	2974	ATCTTTCTAGAAGATCTCCTACAATATTCTCAGCTGCCATGGAAAATCGATGTTCTTCTTTA- TTCTCTCAAGATTTTCAGGCTGTATATTTAAACTTATATTAAGAATATGCTAACCACCTCAT- CAGGAACCGTTGTAGGTGGCGTGGGTTTTCTTGGCAATCGACTCTCATGAAAACACGAGCT- AAATATTCAATATGTTCCCTTGACCAACTTTATCTGCATTTTTTTGAACGAGGTTAGAG- CAAGCTTCAGGAACTGAGACAGGAATTTTATTAATAAAATTTAAATTTTGAAGAAAGTTTCAG- GGTTAATAGCATCCATTTTTGCTTTGCAAGTTCCTCAGCATTCTTAACAAAAGACGCTCTCTT- TTGACATGTTTAAAGTTTAAACCTCTGTGTGAAATTATTATCCGCTCATAATCCACACATT- ATACGAGCCGGAAGCATAAAGTGTAAAGCCTGGGGTGCCTAATGAGTGAGCTAACTCACAT- TAATTGCGTTGCGCTCACTGCCAATTGCTTCCAGTCGGGAAACCTGTCGTGCCAGCTGCATT- AATGAATCGGCCAACGCGCGGGGAGAGGCGGTTTGCCTATTGGGCGCTCTCCGCTTCTCG- CTCACTGACTCGCTGCGCTCGGTCGTTCCGGCTGCGGCGAGCGGTATCAGCTCACTCAAAGGC- GGTAATACGGTTATCCACAGAATCAGGGGATAACGCAGGAAAGAATATGAGCATAAGAAAAGG- CCAGAAAAGGCCAGGAACCGTAAAAAGGCCGCGTTGCTGGCGTTTTTCCATAGGCTCCGC- CCCCCTGACGAGCATCAAAAAATCGACGCTCAAGTCAGAGGTGGCGAAACCCGACAGGAC- TATAAAGATACCAGGCGTTTTCCCCTGGAAGTCCCTCGTGCCTCTCTGTTCCGACCCCTGC- CGCTTACCGGATACCTGTCCGCCTTCTCCCTTCGGGAAAGCGTGGCGCTTCTCATAGCTCAC- GCTGTAGGTATCTCAGTTCGGTGTAGGTCGTTCCGCTCCAAGCTGGGCTGTGTGCACGAACCC- CCGTTTACGCCCAGCCGCTGCGCTTATCCGGTAACTATCGTCTTGAGTCCAACCCGTTAAG- ACACGACTTATCGCCACTGGCAGCAGCCACTGGTAAACAGGATTAGCAGAGCGAGGTATGTA- GGCGGTGCTACAGAGTCTTGAAGTGGTGGCCTAACTACGGCTACACTAGAAGGACAGTAT- TTGGTATCTGCGCTCTGCTGAAGCCAGTTACCTTCGAAAAAGAGTTGGTAGCTCTTGATCC- GGCAAAACAAACCACCGCTGGTAGCGGTGGTTTTTTTGGTTTGAAGCAGCAGATTACGCGCAG- AAAAAAGGATCTCAAGAAGATCCTTTGATCTTTTCTACGGGGTCTGACGCTCAGTGGAAACG- AAAACCTCACGTTAAGGGATTTTGGTTCATGAGATTATCAAAAAGGATCTTACCTAGATCCCTT- TTAAATTAATAAATGAAGTTTAAATCAATCTAAAGTATATATGAGTAAACTTGGTCTGACAG- TTACCAATGCTTAATCAGTGAGGCACCTATCTCAGCGATCTGTCTATTTTCGTTTCCATAGT- TGCTGACTCCCCGTCGTGTAGATAACTACGATACGGGAGGGCTTACCATCTGGCCCCAGTG- CTGCAATGATACCGCGAGACCCACGCTCACCGGCTCCAGATTATCAGCAATAAACCCAGCC- AGCCGGAAGGGCCGAGCGCAGAAGTGGTCTGCAACTTATCCGCCTCCATCCAGTCTATTA- ATTGTTGCGGGAAGCTAGAGTAAGTAGTTCGCCAGTTAATAGTTGCGCAACCGTTGTTGCC- ATTGCTACAGGCATCGTGGTGTACGCTCGTCTTGGTATGGCTTCATTACGCTCCGGTTCC- CAACGATCAAGGCGAGTTACATGATCCCCATGTTGTGCAAAAAAGCGGTTAGCTCCTTCGG- TCTCCGATCGTTGTCAGAAAGTAAAGTTGGCCGAGTGTTATCACTCATGGTTATGGCAGCAC- TGCATAATTCTTACTGTATGCCATCCGTAAGATGCTTTTCTGTGACTGGTGAGTACTCAA- CCAAGTCATTCTGAGAATAGTGTATGCGGCGACCGAGTTGCTCTTGGCCGCGTCAATACGG- GATAATACCGCGCCACATAGCAGAACTTTAAAAGTGCTCATCATTTGAAAAACGTTCTTCGGG- GCGAAAACTCTCAAGGATCTTACCCTGTTGAGATCCAGTTCGATGTAACCCACTCGTGCAC- CCAAGTATCTTACGATCTTTTACTTTACCAGCGTTTCTGGGTGAGCAAAAACAGGAAGG- CAAAATGCCGCAAAAAGGGAATAAGGGCGACACGGAAATGTTGAATACTCATACTCTTCC- TTTTTCAATATTATTGAAGCATTATCAGGGTATTGTCTCATGAGCGGATACATATTTGAAT- GTATTTAGAAAAATAACAAATAGGGGTTCCGCGCACATTTCCCGAAAAGTGCCACCTGA- CGTCTAAGAAAACCATTATTATCATGACATTAACCTATAAAAAATAGCGTATCACGAGGCCGC- CCCTGCAGCCGAATTATATTATTTTGGCCAAATAATTTTTAACAAAAGCTCTGAAGTCTTCTT- CATTTAAATCTTAGATGATACTTCTCATCTGGAAAATGTCCCAATTAGTAGCATCACGCTGTG- AGTAAGTCTAAACCATTTTTTATTGTTGATTATCTCTAATCTTACTACTCGATGAGTTTTC- GGTATTATCTTATTTTAACTTGGAGCAGGTTCCATTCATTGTTTTTTTTCATCATAGTGAATA- AAATCAACTGCTTTAACTTGTGCCTGAACACCATATCCATCCGGCGTAATACGACTCACT- ATAGGGAGAGCGGCCCGCCAGATCTTCCGGATGGCTCGAGTTTTTTCAGCAAGAT

## Oligonucleotides

Supplementary Table S2: Oligonucleotides for the amplification of all toy-model plasmid parts (shown in Figure 1B).<sup>1</sup> The complete part 1 was ordered as oligonucleotides, which were phosphorylated and annealed to double stranded DNA before the LCR (described in the methods).<sup>2</sup> For sequencing from the vector into the inserts. fw: forward direction (5' end), *mRFP1*: monomeric red fluorescent protein 1, rv: reverse direction (3' end), *sfGFP*: superfolder green fluorescent protein.

Toy-Plasmid Part	OligoID	Sequence (5'→3')
<i>mRFP1</i> (Addgene: pYTK090)		
part 1 ( <i>mRFP1</i> -part 1 <sup>1</sup> )	10141-fw	TCCCTATCAGTGATAGAGATTGACATCCCTATCAGTGATAGAGATACTGAGCACGGATCTGAA- AGAGGAGAAAAGGATCT
	10142-rv	AGATCCTTTCCTCTTTTCAGATCCGTGCTCAGTATCTCTATCACTGATAGGGATGCAATCTCT- ATCACTGATAGGGA
part 2 ( <i>mRFP1</i> -part 2)	10127-fw	ATGGCGAGTAGCGAAGACG
	10128-rv	GTCCTGGGTAACGGTAACAAC
part 3 ( <i>mRFP1</i> -part 3)	10129-fw	TCCTCCCTGCAAGACGG
	10132-rv	TATAAACGCAGAAAGGCCAC
<i>sfGFP</i> (Addgene: pYTK001)		
part 4 ( <i>sfGFP</i> -part 1)	10108-fw	GAAAGTGAAACGTGATTTTCATGCG
	10110-rv	TGAACTCAGCGTCAGTTTAC
part 5 ( <i>sfGFP</i> -part 2)	10111-fw	TCTGTACTACTGGTAAACTGC
	10112-rv	TGTGGCTGTAAAATTGTATTCC
part 6 ( <i>sfGFP</i> -part 3)	10113-fw	ATGTTTACATCACCGCCG
	10109-rv	TATAAACGCAGAAAGGCCAC
pJET1.2/blunt		
part 7	23043-fw	ATCTTGCTGAAAAACTCGAGC
	23044-rv	ATCTTTCTAGAAGATCTCC
Sequencing Primers <sup>2</sup>		
forward	14013	CGACTCACTATAGGGAGAGCGGC
reverse	14014	AAGAACATCGATTTTCCATGGCAG

Supplementary Table S3: Oligonucleotides for crosstalk LCRs (results shown in Figures 2 and 3). All melting temperatures ( $T_m$ s) presented here are calculated for each BO-half using the formula of SantaLucia (20) for the  $T_m$ -calculation and the salt correction.  $T_m$ : melting temperature of a BO-half.

Bridging Oligo Set ( $T_m$ per BO-half)	OligoID	Sequence (5'→3')
<b>Manually Designed</b>		
M (71.4±0.7°C)	10133	CGGATGGCTCGAGTTTTTCAGCAAGATTCCTATCAGTGATAGAGATTGACATCCCTATCAG
	10134	GCACGGATCTGAAAGAGGAGAAAGGATCTATGGCGAGTAGCGAAGACGTTATCAAAG
	10135	GTGGTGTGTTACCGTTACCCAGGACTCCTCCCTGCAAGACGGTGAGTTC
	10137	CGGCCGCGTGTACAACCAATGAAAGTGAAACGTGATTTTCATGCGTCATTTTGAAC
	10116	GCAACTAATGGTAAACTGACGCTGAAGTTCATCTGTACTACTGGTAAACTGCCGGTTCC
	10117	CCATAAGCTGGAATACAATTTTAACAGCCACAATGTTTACATCACCGCCGATAAACAAAAAATG
	10118	CGGGTGGGCCTTTCTGCGTTTATAATCTTTCTAGAAGATCTCCTACAATATTCTCAGCTGC
<b>Low Crosstalk</b>		
L1 (68.1±1.1°C)	10232	TGGCTCGAGTTTTTCAGCAAGATTCCTATCAGTGATAGAGATTGACATCC
	10233	CGGATCTGAAAGAGGAGAAAGGATCTATGGCGAGTAGCGAAGACGT
	10234	GTGTTGTTACCGTTACCCAGGACTCCTCCCTGCAAGACGGTG
	10235	GGCCGCGTGTACAACCAATGAAAGTGAAACGTGATTTTCATGCGT
	10236	AATGGTAAACTGACGCTGAAGTTCATCTGTACTACTGGTAAACTGCCGG
	10237	CATAAGCTGGAATACAATTTTAACAGCCACAATGTTTACATCACCGCCGATAAACAAAAA
	10238	CGGGTGGGCCTTTCTGCGTTTATAATCTTTCTAGAAGATCTCCTACAATATTCTCAGC
L2 (68.6±0.9°C)	10235	GGCCGCGTGTACAACCAATGAAAGTGAAACGTGATTTTCATGCGT
	10239	GATGGCTCGAGTTTTTCAGCAAGATTCCTATCAGTGATAGAGATTGACATCCCT
	10240	ACGGATCTGAAAGAGGAGAAAGGATCTATGGCGAGTAGCGAAGACGTTATC
	10241	GGTGTGTTACCGTTACCCAGGACTCCTCCCTGCAAGACGGTG
	10242	CAACTAATGGTAAACTGACGCTGAAGTTCATCTGTACTACTGGTAAACTGCCGG
	10243	ATAAGCTGGAATACAATTTTAACAGCCACAATGTTTACATCACCGCCGATAAACAAAAA
	10244	GGGTGGGCCTTTCTGCGTTTATAATCTTTCTAGAAGATCTCCTACAATATTCTCAGC
L3 (69.5±1.7°C)	10244	GGGTGGGCCTTTCTGCGTTTATAATCTTTCTAGAAGATCTCCTACAATATTCTCAGC
	10268	GGCCGCGTGTACAACCAATGAAAGTGAAACGTGATTTTCATGCGTC
	10283	GGATGGCTCGAGTTTTTCAGCAAGATTCCTATCAGTGATAGAGATTGACATCCC
	10284	GCACGGATCTGAAAGAGGAGAAAGGATCTATGGCGAGTAGCGAAGACGTTATC
	10285	GTGTTGTTACCGTTACCCAGGACTCCTCCCTGCAAGACGGTGAGTTC
	10286	GCAACTAATGGTAAACTGACGCTGAAGTTCATCTGTACTACTGGTAAACTGCCGGT
	10287	TAAGCTGGAATACAATTTTAACAGCCACAATGTTTACATCACCGCCGATAAACAAAAAATGG
L4 (69.4±1.6°C)	10244	GGGTGGGCCTTTCTGCGTTTATAATCTTTCTAGAAGATCTCCTACAATATTCTCAGC
	10268	GGCCGCGTGTACAACCAATGAAAGTGAAACGTGATTTTCATGCGTC
	10283	GGATGGCTCGAGTTTTTCAGCAAGATTCCTATCAGTGATAGAGATTGACATCCC
	10284	GCACGGATCTGAAAGAGGAGAAAGGATCTATGGCGAGTAGCGAAGACGTTATC
	10285	GTGTTGTTACCGTTACCCAGGACTCCTCCCTGCAAGACGGTGAGTTC
	10286	GCAACTAATGGTAAACTGACGCTGAAGTTCATCTGTACTACTGGTAAACTGCCGGT
	10288	TAAGCTGGAATACAATTTTAACAGCCACAATGTTTACATCACCGCCGATAAACAAAAAATG
L5 (69.9±2.1°C)	10235	GGCCGCGTGTACAACCAATGAAAGTGAAACGTGATTTTCATGCGT

Supplementary Table S3: Oligonucleotides for crosstalk LCRs (continued).

Bridging Oligo Set ( $T_m$ per BO-half)	OligoID	Sequence (5' → 3')
L6 (70.0 ± 1.7 °C)	10260	CGGATGGCTCGAGTTTTTCAGCAAGATTCCTATCAGTGATAGAGATTGACATCCCTAT
	10261	CGGATCTGAAAGAGGAGAAAGGATCTATGGCGAGTAGCGAAGACGTTATC
	10262	TGGTGTGTTACCGTTACCCAGGACTCCTCCCTGCAAGACGGTGAGTTC
	10263	GCAACTAATGGTAAACTGACGCTGAAGTTCATCTGTACTACTGGTAAACTGCCGGTTCCTT
	10264	TAAGCTGGAATACAATTTTAACAGCCACAATGTTTACATCACCGCCGATAAACA
	10265	GGGTGGCCCTTTCTGCGTTTATAATCTTTCTAGAAGATCTCTACAATATTCTCAGCTGCC
	10259	GTGGTGTGTTACCGTTACCCAGGACTCCTCCCTGCAAGACGGTGAGTT
	10266	CGGATGGCTCGAGTTTTTCAGCAAGATTCCTATCAGTGATAGAGATTGACATCCCTA
	10267	CGGATCTGAAAGAGGAGAAAGGATCTATGGCGAGTAGCGAAGACGTT
	10268	GGCCGCGTGTTACAACCAATGAAAGTGAAACGTGATTTTCATGCGTC
	10269	CAACTAATGGTAAACTGACGCTGAAGTTCATCTGTACTACTGGTAAACTGCCGGT
	10270	GCCATAAGCTGGAATACAATTTTAACAGCCACAATGTTTACATCACCGCCGATAAACA
10271	TTCGGGTGGCCCTTTCTGCGTTTATAATCTTTCTAGAAGATCTCTACAATATTCTCAGCT	
<b>High Crosstalk</b>		
H1 (71.9 ± 1.1 °C)	10245	CGGATGGCTCGAGTTTTTCAGCAAGATTCCTATCAGTGATAGAGATTGACATCCCTATCAGT
	10246	GCACGGATCTGAAAGAGGAGAAAGGATCTATGGCGAGTAGCGAAGACGTTATCAAAG
	10247	GTGGTGTGTTACCGTTACCCAGGACTCCTCCCTGCAAGACGGTGAGT
	10248	GCGGCCGCGTGTTACAACCAATGAAAGTGAAACGTGATTTTCATGCGTCATTTGAACA
	10249	CAACTAATGGTAAACTGACGCTGAAGTTCATCTGTACTACTGGTAAACTGCCGGTTCCTT
	10250	GCCATAAGCTGGAATACAATTTTAACAGCCACAATGTTTACATCACCGCCGATAAACA
	10251	TTCGGGTGGCCCTTTCTGCGTTTATAATCTTTCTAGAAGATCTCTACAATATTCTCAGCTGCC
	H2 (70.7 ± 2.4 °C)	10248
10252		ATGGCTCGAGTTTTTCAGCAAGATTCCTATCAGTGATAGAGATTGACATCCCTATCAGT
10253		AGCACGGATCTGAAAGAGGAGAAAGGATCTATGGCGAGTAGCGAAGACGTT
10254		GTGGTGTGTTACCGTTACCCAGGACTCCTCCCTGCAAGACGGTGAGTTC
10255		AATGGTAAACTGACGCTGAAGTTCATCTGTACTACTGGTAAACTGCCGGTTCCTT
10256		AAGCTGGAATACAATTTTAACAGCCACAATGTTTACATCACCGCCGATAAACA
10257		TTCGGGTGGCCCTTTCTGCGTTTATAATCTTTCTAGAAGATCTCTACAATATTCTCAGCTG
H3 (70.3 ± 2.3 °C)	10248	GCGGCCGCGTGTTACAACCAATGAAAGTGAAACGTGATTTTCATGCGTCATTTGAACA
	10265	GGGTGGCCCTTTCTGCGTTTATAATCTTTCTAGAAGATCTCTACAATATTCTCAGCTGCC
	10289	GATGGCTCGAGTTTTTCAGCAAGATTCCTATCAGTGATAGAGATTGACATCCCTATCA
	10290	AGCACGGATCTGAAAGAGGAGAAAGGATCTATGGCGAGTAGCGAAGACGTTA
	10291	GTGGTGTGTTACCGTTACCCAGGACTCCTCCCTGCAAGACGGTG
	10292	AATGGTAAACTGACGCTGAAGTTCATCTGTACTACTGGTAAACTGCCGGTTC
H4 (70.5 ± 2.2 °C)	10293	GCCATAAGCTGGAATACAATTTTAACAGCCACAATGTTTACATCACCGCCGATAAACA
	10248	GCGGCCGCGTGTTACAACCAATGAAAGTGAAACGTGATTTTCATGCGTCATTTGAACA
	10265	GGGTGGCCCTTTCTGCGTTTATAATCTTTCTAGAAGATCTCTACAATATTCTCAGCTGCC
	10290	AGCACGGATCTGAAAGAGGAGAAAGGATCTATGGCGAGTAGCGAAGACGTTA
	10291	GTGGTGTGTTACCGTTACCCAGGACTCCTCCCTGCAAGACGGTG

Supplementary Table S3: Oligonucleotides for crosstalk LCRs (continued).

<b>Bridging Oligo Set (<math>T_m</math> per BO-half)</b>	<b>OligoID</b>	<b>Sequence (5'→3')</b>
H5 (70.4±1.9°C)	10292	AATGGTAAACTGACGCTGAAGTTCATCTGTACTACTGGTAAACTGCCGGTTC
	10293	GCCATAAGCTGGAATACAATTTTAACAGCCACAATGTTTACATCACCGCCGATAAACA
	10294	CGGATGGCTCGAGTTTTTCAGCAAGATTCCTATCAGTGATAGAGATTGACATCCCTATCA
	10248	GCGGCCGCGTGTTACAACCAATGAAAGTGAAACGTGATTTTCATGCGTCATTTTGAACA
	10272	TGGCTCGAGTTTTTCAGCAAGATTCCTATCAGTGATAGAGATTGACATCCCTATCAGT
	10273	CACGGATCTGAAAGAGGAGAAAGGATCTATGGCGAGTAGCGAAGACGTTATCAAAGA
	10274	GTGTTGTTACCGTTACCCAGGACTCCTCCCTGCAAGACGGTGA
	10275	CAACTAATGGTAAACTGACGCTGAAGTTCATCTGTACTACTGGTAAACTGCCGGTTC
H6 (70.3±2.2°C)	10276	CATAAGCTGGAATACAATTTTAACAGCCACAATGTTTACATCACCGCCGATAAACAATAATGG
	10277	CGGGTGGGCCTTTCTGCGTTTATAATCTTTCTAGAAGATCTCCTACAATATTCTCAGCTG
	10242	CAACTAATGGTAAACTGACGCTGAAGTTCATCTGTACTACTGGTAAACTGCCGG
	10248	GCGGCCGCGTGTTACAACCAATGAAAGTGAAACGTGATTTTCATGCGTCATTTTGAACA
	10278	GATGGCTCGAGTTTTTCAGCAAGATTCCTATCAGTGATAGAGATTGACATCCCTATCAGT
	10279	AGCACGGATCTGAAAGAGGAGAAAGGATCTATGGCGAGTAGCGAAGACGTTATCAA
	10280	GTGGTGTGTTACCGTTACCCAGGACTCCTCCCTGCAAGACGGTGA
	10281	AGCTGGAATACAATTTTAACAGCCACAATGTTTACATCACCGCCGATAAACAA
10282	TTCGGGTGGGCCTTTCTGCGTTTATAATCTTTCTAGAAGATCTCCTACAATATTCTCAGC	



Supplementary Table S4: Bridging oligo sets for the gradient-LCR (composed of bridging oligos for crosstalk experiments; Supplementary Table S3). The results of the gradient-LCRs are shown in Figure 4A+B. All melting temperatures ( $T_m$ s) presented here are calculated for each BO-half using the formula of SantaLucia (20) for the  $T_m$ -calculation and the salt correction.  $T_m$ : melting temperature of a BO-half.

Bridging Oligo Set ( $T_m$ per BO-half)	OligoID	Sequence (5'→3')
67.8±0.5°C	10232	TGGCTCGAGTTTTTCAGCAAGATTCCTATCAGTGATAGAGATTGACATCC
	10233	CGGATCTGAAAGAGGAGAAAGGATCTATGGCGAGTAGCGAAGACGT
	10234	GTGTTGTTACCGTTACCCAGGACTCCTCCCTGCAAGACGGTG
	10236	AATGGTAACTGACGCTGAAGTTCATCTGTACTACTGGTAACTGCCGG
	10244	GGGTGGGCCTTTCTGCGTTTATAATCTTTCTAGAAGATCTCCTACAATATTCTCAGC
	10268	GGCCGCGTGTACAACCAATGAAAGTAAACGTGATTTTCATGCGTC
	10281	AGCTGGAATACAATTTTAACAGCCACAATGTTTACATCACCGCCGATAAAACAA
	69.9±1.3°C	10117
10118		CGGGTGGGCCTTTCTGCGTTTATAATCTTTCTAGAAGATCTCCTACAATATTCTCAGCTGC
10240		ACGGATCTGAAAGAGGAGAAAGGATCTATGGCGAGTAGCGAAGACGTTATC
10247		GTGGTGTGTTACCGTTACCCAGGACTCCTCCCTGCAAGACGGTGAGT
10268		GGCCGCGTGTACAACCAATGAAAGTAAACGTGATTTTCATGCGTC
10269		CAACTAATGGTAAACTGACGCTGAAGTTCATCTGTACTACTGGTAACTGCCGGTT
10283		GGATGGCTCGAGTTTTTCAGCAAGATTCCTATCAGTGATAGAGATTGACATCCC
71.8±0.8°C		10116
	10117	CCATAAGCTGGAATACAATTTTAACAGCCACAATGTTTACATCACCGCCGATAAAACAAAAAATG
	10133	CGGATGGCTCGAGTTTTTCAGCAAGATTCCTATCAGTGATAGAGATTGACATCCCTATCAG
	10134	GCACGGATCTGAAAGAGGAGAAAGGATCTATGGCGAGTAGCGAAGACGTTATCAAAG
	10248	GCGGCCGCGTGTACAACCAATGAAAGTAAACGTGATTTTCATGCGTCATTTTGAACA
	10251	TTCGGGTGGGCCTTTCTGCGTTTATAATCTTTCTAGAAGATCTCCTACAATATTCTCAGCTGCC
	10259	GTGGTGTGTTACCGTTACCCAGGACTCCTCCCTGCAAGACGGTGAGTT

Supplementary Table S5: Bridging oligo sets with temperatures in the range of 62.0 °C to 67 °C. The results of the LCRs are shown in Figure 4C+D. All melting temperatures ( $T_m$ s) presented here are calculated for each BO-half using the formula of SantaLucia (20) for the  $T_m$ -calculation and the salt correction.  $T_m$ : melting temperature of a BO-half.

Bridging Oligo Set ( $T_m$ per BO-half)	OligoID	Sequence (5'→3')
62.0±0.9°C	10331	GGAATACAATTTTAACAGCCACAATGTTTACATCACCGCCG
	10333	GCTCGAGTTTTTCAGCAAGATTCCCTATCAGTGATAGAGATTGAC
	10334	ATCTGAAAGAGGAGAAAGGATCTATGGCGAGTAGCGAAGAC
	10335	TGTTACCGTTACCCAGGACTCCTCCCTGCAAGACG
	10336	CCGCGTGTACAACCAATGAAAGTAAAACGTGATTTTCATGC
	10337	AAACTGACGCTGAAGTTCATCTGTACTACTGGTAAACTGC
	10338	GGGCCTTTCTGCGTTTATAATCTTTCTAGAAGATCTCCTACAATAT
	10333	GCTCGAGTTTTTCAGCAAGATTCCCTATCAGTGATAGAGATTGAC
63.3±0.7°C	10336	CCGCGTGTACAACCAATGAAAGTAAAACGTGATTTTCATGC
	10339	GATCTGAAAGAGGAGAAAGGATCTATGGCGAGTAGCGAAGAC
	10340	GTTGTTACCGTTACCCAGGACTCCTCCCTGCAAGACGG
	10341	GTAAACTGACGCTGAAGTTCATCTGTACTACTGGTAAACTGCC
	10342	TGGAATACAATTTTAACAGCCACAATGTTTACATCACCGCCGATA
	10343	TGGGCCTTTCTGCGTTTATAATCTTTCTAGAAGATCTCCTACAATATTCT
	10340	GTTGTTACCGTTACCCAGGACTCCTCCCTGCAAGACGG
65.1±0.6°C	10344	GGCTCGAGTTTTTCAGCAAGATTCCCTATCAGTGATAGAGATTGACATC
	10345	GGATCTGAAAGAGGAGAAAGGATCTATGGCGAGTAGCGAAGACG
	10346	GCCGCGTGTACAACCAATGAAAGTAAAACGTGATTTTCATGCG
	10347	GGTAAACTGACGCTGAAGTTCATCTGTACTACTGGTAAACTGCCG
	10348	CTGGAATACAATTTTAACAGCCACAATGTTTACATCACCGCCGATAAA
	10349	GTGGGCCTTTCTGCGTTTATAATCTTTCTAGAAGATCTCCTACAATATTCTC
	10344	GGCTCGAGTTTTTCAGCAAGATTCCCTATCAGTGATAGAGATTGACATC
	10345	GGATCTGAAAGAGGAGAAAGGATCTATGGCGAGTAGCGAAGACG
	10346	GCCGCGTGTACAACCAATGAAAGTAAAACGTGATTTTCATGCG
66.0±0.5°C	10350	TGTTGTTACCGTTACCCAGGACTCCTCCCTGCAAGACGGT
	10351	TGGTAAACTGACGCTGAAGTTCATCTGTACTACTGGTAAACTGCCG
	10352	GCTGGAATACAATTTTAACAGCCACAATGTTTACATCACCGCCGATAAAC
	10353	GGTGGGCCTTTCTGCGTTTATAATCTTTCTAGAAGATCTCCTACAATATTCTCAG
	10350	TGTTGTTACCGTTACCCAGGACTCCTCCCTGCAAGACGGT
	10353	GGTGGGCCTTTCTGCGTTTATAATCTTTCTAGAAGATCTCCTACAATATTCTCAG
	10354	ATGGCTCGAGTTTTTCAGCAAGATTCCCTATCAGTGATAGAGATTGACATCC
67.3±0.6°C	10355	CGGATCTGAAAGAGGAGAAAGGATCTATGGCGAGTAGCGAAGACGT
	10356	GGCCGCGTGTACAACCAATGAAAGTAAAACGTGATTTTCATGCGTC
	10357	CTAATGGTAAACTGACGCTGAAGTTCATCTGTACTACTGGTAAACTGCCGG
	10358	GCTGGAATACAATTTTAACAGCCACAATGTTTACATCACCGCCGATAAACA

Supplementary Table S6: Oligonucleotides for the assembly of the three-part toy-plasmid consisting of *mRFP1*, *sfGFP* and pJET1.2/blunt (results shown in Supplementary Figure S13). Both sets presented here consist of used sets for the LCR optimizations. The BO-set for the baseline LCR consists of BOs of the manual set shown in Supplementary Table S3. The BO-set for the improved LCR consists of BOs of the "67.8 °C"-set of the gradient-LCR (Supplementary Table S4). All melting temperatures ( $T_m$ s) presented here are calculated for each BO-half using the formula of SantaLucia (20) for the  $T_m$ -calculation and the salt correction.  $T_m$ : melting temperature of a BO-half.

<b>Bridging Oligo Set (<math>T_m</math> per BO-half)</b>	<b>OligoID</b>	<b>Sequence (5'→3')</b>
Baseline ( $71.4 \pm 0.6^\circ\text{C}$ )	10133	CGGATGGCTCGAGTTTTTCAGCAAGATTCCTATCAGTGATAGAGATTGACATCCCTATCAG
	10137	CGGCCGCGTGTTACAACCAATGAAAGTGAAACGTGATTTTCATGCGTCATTTTGAAC
	10118	CGGGTGGGCCTTTCTGCGTTTATAATCTTTCTAGAAGATCTCCTACAATATTCTCAGCTGC
Improved ( $67.9 \pm 0.7^\circ\text{C}$ )	10232	TGGCTCGAGTTTTTCAGCAAGATTCCTATCAGTGATAGAGATTGACATCC
	10244	GGGTGGGCCTTTCTGCGTTTATAATCTTTCTAGAAGATCTCCTACAATATTCTCAGC
	10268	GGCCGCGTGTTACAACCAATGAAAGTGAAACGTGATTTTCATGCGTC

# Step-by-step protocol for the ligase cycling reaction

Niels SCHLICHTING, Felix REINHARDT, Sven JAGER, Michael SCHMIDT, Johannes KABISCH

## Abstract

The ligase cycling reaction (LCR) is a scarless and efficient method to assemble plasmids from fragments of DNA. This assembly method is based on the hybridization of DNA fragments with complementary oligonucleotides, so-called bridging oligos (BOs), and an experimental procedure of thermal denaturation, annealing and ligation. In this study, we explore the effect of molecular crosstalk of BOs and various experimental parameters on the LCR by utilizing a fluorescence-based screening system. The results indicate an impact of the melting temperatures of BOs on the overall success of the LCR assembly. Secondary structure inhibitors, such as DMSO and betaine, are necessary for assemblies made of large parts (>350 bp) whereas they show negative effects for assemblies with mixtures of small and large parts. Adjustments of the annealing, ligation and BO-melting temperature are useful but depend on the sizes of the DNA fragments. Based on this, a step-by-step protocol is offered within this study to ensure a transferable routine for high efficient LCR assemblies.

- Reagents**
- amplification of DNA fragments:
    - \* proof-reading polymerase, no T/A overhangs
    - \* phosphorylated primers for the amplification of DNA fragments (use T4-polynucleotide kinase (T4-PNK; New England Biolabs, Ipswich, USA) and T4-PNK buffer (10×) or order as synthetically modified oligos
  - LCR:
    - \* Ampligase<sup>®</sup> thermostable DNA (Lucigen, Wisconsin, USA) ligase (Epicentre) and 10×-buffer
    - \* 100 % DMSO
    - \* 4.5 M betaine
    - \* *aq. dest.*
    - \* competent cells

## Amplification of DNA fragments

- use phosphorylated amplification primers for the amplification of DNA fragments (do not phosphorylate the bridging oligos!)
- phosphorylation of the amplification primers by T4-PNK (on ice):
  - 0.5  $\mu\text{L}$  of 100  $\mu\text{M}$  primer 1  $\mu\text{M}$  (low concentration of primer is more efficient)
  - + 5  $\mu\text{L}$  10 $\times$  T4-PNK buffer (1x)
  - + 1  $\mu\text{L}$  10 000 U ml<sup>-1</sup> T4-PNK (10 U)
  - + 1  $\mu\text{L}$  100 mM ATP (2 mM)
  - + 42.5  $\mu\text{L}$  *aq. dest/MilliQ*
  - $\Sigma$  50  $\mu\text{L}$  of 1  $\mu\text{M}$  primer
- incubate for 1 h at 37 °C and 20 min at 65 °C
- use 12.5  $\mu\text{L}$  of each phosphorylated amplification primer in 50  $\mu\text{L}$  PCR (primer concentration in PCR: 250 nM)
- Recommended: gel extraction of all parts; DpnI digestion of all parts
- store parts at -20 °C; prepare aliquots for multiple usage of the same part (loss of function due to repeated freeze-thaw cycles [1, 2])

## Bridging Oligo Design

In general, the usage of 8% – v/v DMSO and 0.45 M betaine is recommended as a general assembly routine. For this, the target  $T_m$  strongly depends on the utilized algorithms.

general instructions:

- design bridging oligos (BOs) in forward direction
- adjust concentrations:
  - \* salt: 10 mM Mg<sup>2+</sup>, 50 mM Na<sup>+</sup>
  - \* DNA: 3 nM of DNA parts, 30 nM of bridging oligos
  - \* 0 mM dNTPs (has to be adjusted to 0)
- a G or C at the 5'-or 3'-end is not necessary
- to order the BOs as salt-free oligonucleotides is sufficient
- target  $T_m$  of each half (figure 1) depends on utilized algorithms
- in case of too high/low deviation in comparison to the target- $T_m$  choose the higher temperature

Target  $T_m$  for LCRs with DMSO and betaine:

- SantaLucia 1998 ( $T_m$  calculation and salt correction [3])
  - \* target  $T_m = 74.8^\circ\text{C}$

- SantaLucia 1998 ( $T_m$  calculation [3]) and Owczarzy 2008 (salt correction [4])
  - \* target  $T_m = 72.2^\circ\text{C}$
- **Geneious** (www.geneious.com, [5]) utilizing **Primer3** [6]:
  - \* restrictions in adjusting parameters for DNA-part concentration (only "Oligo" can be adjusted)
  - \* to get correct melting temperatures use 114 nM for the input of "Oligo"
  - \* then use SantaLucia 1998 [3] for the  $T_m$  calculation and salt correction (Owczarzy 2008 [4] is not available for the in-house calculations in **Geneious** versions  $\leq 11.0.5$ )
  - \* target  $T_m = 74.8^\circ\text{C}$

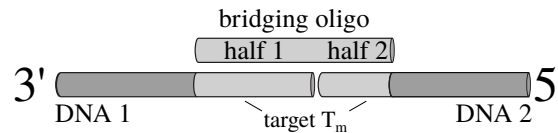


Figure 1: Scheme of the bridging oligo design. Half 1: 100% complementary to the 5-end of the first DNA part. Half 2: 100% complementary to the 3-end of the second DNA part.

For LCRs where small DNA parts are involved ( $<350$  bp) the omission of DMSO/betaine was beneficial. Additionally, the target- $T_m$  is lower in comparison to LCRs with DMSO and betaine and an increase of the annealing temperature from  $55$  to  $66^\circ\text{C}$  was advantageous for the total amount of CFUs.

Target  $T_m$  for LCRs without DMSO and betaine and LCRs where small parts are included:

- SantaLucia 1998 ( $T_m$  calculation and salt correction [3])
  - \* target  $T_m = 67.8^\circ\text{C}$
- SantaLucia 1998 ( $T_m$  calculation [3]) and Owczarzy 2008 (salt correction [4])
  - \* target  $T_m = 65.2^\circ\text{C}$
- **Geneious** (www.geneious.com, [5]) utilizing **Primer3** [6]:
  - \* restrictions in adjusting parameters for DNA-part concentration (only "Oligo" can be adjusted)
  - \* to get correct melting temperatures use 114 nM for the input of "Oligo"



- \* then use SantaLucia 1998 [3] for the  $T_m$  calculation and salt correction (Owczarzy 2008 [4] is not available for the in-house calculations in **Geneious** versions  $\leq 11.0.5$ )
- \* target  $T_m = 67.8^\circ\text{C}$

- Ligation**
- use inserts:vector ratio of 10:1 (use 0.3 nM of vector instead of 3 nM) to reduce the background (religation of the vector occurs due to the phosphorylation of ALL parts in this method)
  - for 25  $\mu\text{l}$  (in brackets: final concentration):
    - DNA inserts (3 nM of each fragment)
    - + vector (0.3 nM)
    - + 0.5  $\mu\text{L}$  of each 1.5  $\mu\text{M}$  bridging oligo (30 nM of each oligo)
    - + 2.5  $\mu\text{L}$  10 $\times$  Ampligase<sup>®</sup> buffer
    - ( + 1.25  $\mu\text{L}$  of 10 mM NAD<sup>+</sup> (0.5 mM) )<sup>1</sup>
    - ( + 2.5  $\mu\text{L}$  of 4.5 M betaine (0.45 M) )
    - ( + 2.0  $\mu\text{L}$  of 100 %-DMSO )(8% – v/v )
    - + 1.5  $\mu\text{L}$  of 5 U  $\mu\text{L}^{-1}$  Ampligase<sup>®</sup> (1.5 U)
    - fill up with *aq. dest* to 25  $\mu\text{L}$
  - use low-profile tubes or low-profile PCR plates (96-well) in a cycler for volumes of less than 10  $\mu\text{L}$
  - for more than 25 cycles of small volumes ( $\leq 5 \mu\text{L}$ ): use 384-well plates
  - start cycling (figure 2)

Initial denaturation :	94°C	2 min	
Denaturation :	94°C	10 s	} 25-50x
Annealing :	55/66°C	30 s	
Ligation :	66°C	1 min	
Hold :	10°C	$\infty$	

Figure 2: Cycling parameters for the LCR. For DMSO/betaine-free LCRs use the annealing temperature of 66 °C.

- store at  $-20^\circ\text{C}$  or directly use for transformation of chemically- or electrocompetent cells or use LCR-mix as template in a PCR (1  $\mu\text{l}$  of 1:100 dilution works in general)
- if DMSO+betaine is utilized for the LCR in the combination with electroporation: performing a dialysis increases the amount of colonies (30 min using a floating membrane in a Petri dish filled with *aq. dest.*)

- Notes**
1. Self-made 10 $\times$ -buffer without NAD<sup>+</sup> is recommended. NAD<sup>+</sup> is sensitive to freeze-thaw cycles, long-term storage and light exposure. Prepare a stock solution of NAD<sup>+</sup> and store in aliquots at  $-80^\circ\text{C}$  up to 6 months. 10 $\times$  Ampligase<sup>®</sup> buffer: 200 mM TRIS-HCl (pH 8.3), 250 mM KCl, 100 mM MgCl<sub>2</sub>, 0.1% Triton X-100.

## References

- [1] Robinson, C. J., Dunstan, M. S., Swainston, N., Titchmarsh, J., Takano, E., Scrutton, N. S., and Jervis, A. J. (January, 2018) Chapter Thirteen - Multifragment DNA Assembly of Biochemical Pathways via Automated Ligase Cycling Reaction. In Scrutton, N., (ed.), *Methods in Enzymology*, Vol. 608 of Enzymes in synthetic biology, pp. 369–392 Academic Press.
- [2] Davis, D. L., O’Brie, E. P., and Bentzley, C. M. (October, 2000) Analysis of the degradation of oligonucleotide strands during the freezing/thawing processes using MALDI-MS. *Analytical Chemistry*, **72**(20), 5092–5096.
- [3] SantaLucia, J. (February, 1998) A unified view of polymer, dumbbell, and oligonucleotide DNA nearest-neighbor thermodynamics. *Proceedings of the National Academy of Sciences*, **95**(4), 1460–1465.
- [4] Owczarzy, R., Moreira, B. G., You, Y., Behlke, M. A., and Walder, J. A. (May, 2008) Predicting stability of DNA duplexes in solutions containing magnesium and monovalent cations. *Biochemistry*, **47**(19), 5336–5353.
- [5] Kearse, M., Moir, R., Wilson, A., Stones-Havas, S., Cheung, M., Sturrock, S., Buxton, S., Cooper, A., Markowitz, S., Duran, C., Thierer, T., Ashton, B., Meintjes, P., and Drummond, A. (June, 2012) Geneious basic: an integrated and extendable desktop software platform for the organization and analysis of sequence data. *Bioinformatics*, **28**(12), 1647–1649.
- [6] Untergasser, A., Cutcutache, I., Koressaar, T., Ye, J., Faircloth, B. C., Remm, M., and Rozen, S. G. (August, 2012) Primer3-new capabilities and interfaces. *Nucleic Acids Research*, **40**(15), e115.